THESIS REPORT
Master's Degree

SYSTEMS
RESEARCH
CENTER

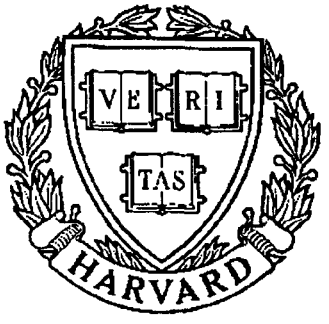

Supported by the National Science Foundation Engineering Research Center Program (NSFD CD 8803012), Industry and the University

Tactile Perception for Multifingered Hands

by : R. Yang
Advisor: P.S. Krishnaprasad

M.S. 87-6
Formerly TR 87-162

APPROVAL SHEET

Title of Thesis: Tactile Perception for Multifingered Hands

Name of Candidate: Rui Yang

Master of Science, 1987

Thesis and Abstract Approved:

Dr. P. S. Krishnaprasad

Professor

Department of Electrical Engineering

Data Approved:

ABSTRACT

Title of Thesis: Tactile Perception for Multifingered Hands

Rui Yang, Master of Science, 1987

Thesis directed by: P. S. Krishnaprasad

Professor

Department of Electrical Engineering

Recently, tactile sensors mounted on robot fingers have been identified as essential sensory devices for the control of multifingered robotic hands. A basic tactile sensing task is to determine the force distribution on the contact area between the fingers and grasped object. To increase the grasp stability and to protect the fragile sensors, a kind of elastic material is required to cover the tactile sensors. This thesis derives the relationship between the surface force profile and the stress or strain profile measured by tactile sensors beneath the contact surface for simplified situations. This relationship can be described by integral equations of convolution type, or more generally, integral equations of the first kind with two unknown functions. The algorithms for numerical inversion of such equations are derived by using the techniques of Discrete Fourier Transformation and Regularization. Several examples are given. To realize the inversion in real time, an analog network for solving the regularization problem is discussed. Finally, as an application of the tactile sensors, the equilibrium condition for stable grasping by a two-fingered robotic hand is derived.

TACTILE PERCEPTION FOR MULTIFINGERED HANDS

by

Rui Yang

Thesis submitted to the Faculty of the Graduate School
of the University of Maryland in partial fulfillment
of the requirements for the degree of
Master of Science
1987

Advisory Committee:

Professor P. S. Krishnaprasad
Professor J. Baras
Associate Professor M. Shayman

© Copyright by

Rui Yang

1987

ACKNOWLEDGMENTS

I wish to thank my professors who have contributed suggestions for my thesis. In particular, I thank Dr. P. S. Krishnaprasad, my advisor, for his inspiration and encouragement throughout my research and for his patient guidance in my writing and correcting the thesis. I also wish to thank the other members of the thesis committee, Dr. J. Baras and Dr. M. Shayman for their help. I would like to acknowledge the support from the Systems Research Center (SRC) through a fellowship. And I appreciate very much the patience and consideration I have been shown by my many friends and associates along the way.

TABLE OF CONTENTS

Acknowledgements ii

Table of Contents iii

List of Figures iv

Chapter 1. Introduction 1

Chapter 2. The Model of the Elastic Material and Some Assumptions 5
2.1 The Expression for Stress due to Surface Contact 6
2.2 The Expression for Strain due to Surface Contact 8
2.3 Some Assumptions 11

Chapter 3. The DFT Approach to the Inverse Problem 15
3.1 Surface Force Profile without Tangential Component 15
3.2 Surface Force Profile with Tangential Component 21
3.3 Examples 24

Chapter 4. The Regularization for the Inverse Problem 33
4.1 The Concept of Ill-posed Problem 33
4.2 The Regularization Approach 36
4.3 An Algorithm to Solve the Equation of First Kind 39
4.4 An Algorithm for the Inverse Problem with Two Unknown Functions 44
4.5 Examples 50

Chapter 5. Analog Networks for the Inverse Problem 55
5.1 Equivalence of Analog Networks and Regularization 55
5.2 Analog Networks for The Inverse Problem 61

Chapter 6. An Application of Tactile Sensors in Statics of Multifingered Hand 65
6.1 Definitions and Assumptions 65
6.2 The Concept of Concentrated Contact Force 66
6.3 The Statics Problem in a Multifingered Hand System 69

Chapter 7. Conclusion 76
Bibliography 78

LIST OF FIGURES

2.1 Line force on elastic half-plane 7
2.2 The kernels expressed by stress 9
2.3 The kernels expressed by strain 12
3.1 The Fourier transform of K_1^{stress} 17
3.2 The Fourier transform of K_1^{strain} 18
3.3 The DFT of K_1^{stress} 19
3.4 The DFT of K_1^{strain} 20
3.5 Cylindrical and rectangular indentor 25
3.6 Reconstruction of surface stress for cylindrical indenting, $f_t = 0$ 26-28
3.7 Reconstruction of surface stress for rectangular indenting, $f_t \neq 0$ 29-30
3.8 The comparison of the reconstruction for different measurements 31-32
4.1 Reconstruction of surface stress for cylindrical indenting, $f_t = 0$ 51-52
4.2 Reconstruction of surface stress for cylindrical indenting, $f_t \neq 0$ 53-54
5.1 A simple network for solving the inverse problem 64
6.1 Surface contact and its equivalent point contact 66
6.2 Two finger grasping 70

CHAPTER
ONE

INTRODUCTION

Today's robots are required to perform increasingly more sophisticated tasks. Different kinds of robotic hands or 'end effectors', which play a role as the interface between the mechanical arm and the environment, have been designed. The structures of these hands as developed for manipulation tasks range from simple gripper designs to multifingered and articulated hands. In order to implement feedback control of such hands, the need for robotic sensing capability becomes evident.

Historically, vision has been the dominant area of robotic sensory perception research. Vision is important since it is the main sensing tool for an intelligent robot to determine the strategies of motion such as object identification for motion guidance and obstacle avoidance for motion trajectories. However, for many applications in hand control, the sense of touch is often considered more important during manipulation. For example, a robot should be able to know the moment of contact between the robotic fingers and grasped object. A robot should also be able to determine how much grasping force is being exerted upon that object so that the grasp is stable, i.e. there exists no sliding and excess force between the object and fingers.

Unlike simple touching, or binary sensing, which includes only two possible states, tactile sensing can be defined as the continuous sensing of a variable contact force, commonly by an array of sensors. This sensing should be capable of being performed within an arbitrary three dimensional space. This generally refers to skinlike properties where areas of force-sensitive and displacement-sensitive surfaces are capable of graded signals and parallel patterns of touching.

Continuously variable analog sensors have been the subject of much research for a long time. Most of these sensors have relied upon the generation of electric signals resulting from the deformation of some force-sensitive material. These materials have included resistive paints, conductive rubbers and polymers, piezo-electric materials, and semiconductor strain gages. There are two key features of most sensor designs:

1. To achieve high sensitivity, the sensor structure is often very weak and fragile so that they cannot directly endure high pressure on them.

2. The operating principle for sensors based on these materials is that a progressive deformation of such material causes a measurable, monotonic change in electrical resistance. The information measured by such sensors can not however be used directly.

In practice, when a rigid object which has a sharp boundary, e.g. a wedge, is grasped by the robotic hand, very high pressure is developed at the contact area. This can be illustrated by noticing that after pressing a coin on the palm of human hand, an indentation appears on the hand due to the edge of the coin. A common method to avoid damaging the sensors is to use an elastic material to cover the tactile sensors. This method is effective since the intensity of the exerted force is reduced and distributed within the material. This is the

first process of tactile sensing, called transduction which converts the feature of contact signals into another form, e.g. the interior strain of elastic material.

On the other hand, the relation between the contact force profile and the strain profile which is measured beneath the surface needs to be established, and an approach to solve the surface force profile from this relation should be obtained. This is the second process of tactile sensing, called data processing which translates the measured signals into useful information. The main part of this thesis deals with these problems.

In addition, when the tactile sensors are mounted on the finger tip of a hand, and the the distribution of contact force is reconstructed, it is a fundamental problem to design a control system to use tactile feedback. This thesis will consider the condition of stable grasping when the robotic hand is in equilibrium state. This condition may be one of the criteria for control system to achieve.

In chapter 2, applying the theory of elasticity for a simplified situation, we derive the relation between the surface load and the distribution of stress or strain beneath the surface. We find that this relation can be described by an integral equation of convolution type. By decomposing the distribution of surface force into vertical and tangential components, this equation generally has two unknown functions. Since the unknown functions are convolved , solving for them from the observations and the property of elastic material will be referred to as *the inverse problem.* In chapter 3, by considering the property of convolution and spatially discrete form of observation, we use the Discrete Fourier Transformation(DFT) approach to solve the inverse problem approximately. Since the integral equation can be considered as an operator equation of the first kind in a more general sense, in chapter 4, we apply the regularization approach to solve the inverse problem. Several examples are given in

both chapter 3 and chapter 4. By observing that, if the calculations are carried out by a digital computer, both approaches above are not suitable for real time control, in chapter 5, we investigate an approach by based on an analog network for regularization. In chapter 6, we study the condition of equilibrium for a two-fingered hand which is grasping an object. An external force is exerted on the gasped object. In this condition, the contact information reconstructed by tactile sensors is applied. Finally, in chapter 7, we review the thesis and give suggestions for further research.

CHAPTER
TWO

THE MODEL OF THE ELASTIC MATERIAL AND SOME ASSUMPTIONS

In this chapter, we attempt to find the relation between the load profile, which exists on the surface of a half space of elastic material, and the distribution of stress or strain beneath the surface of that material. To specify the load, we shall just consider the contact stress profile rather than the contact displacement profile for the following reasons:

- The contact stress is more directly useful for stable grasping. (see, Chapter 6)
- There is a complex nonlinear relation between displacement profile and surface stress profile.(Phillips and Johnson, 1981)

We assume that the dimension of the contact area is infinitely large in a direction, say z, such as a line load. By this assumption, we just need to analyze two dimensional behavior in a slice perpendicular to that direction. We also assume that the elastic characteristics of the material are homogeneous and isotropic. From the theory of elasticity (Timoshenko and Goodier, 1951), under this assumption, the differential equation of the equilibrium, the boundary condition and the condition of compatibility for the stress are linear. Consequently,

it is possible to consider the interior stress or strain distribution due to a general contact as the superposition of those quantities due to a set of line contacts.

2.1 The Expression of Stress due to Surface Contact

We now study the behavior of an infinite homogeneous and isotropic elastic material under a line contact with negligible contact width. From the theory of elasticity for two dimensional problems in polar coordinates(Timoshenko and Goodier, 1951), the distribution of stress follows a simple radial distribution. For the concentrated force inclined from the vertical by an angle, $\alpha(< \pi/2)$, we have

$$\sigma_r = \frac{2f\cos(\theta - \alpha)}{\pi r}$$

$$\sigma_\theta = 0$$

$$\tau_{r\theta} = 0$$

where σ_r is the radial stress at the point (r, θ), σ_θ is the stress in the plane at (r, θ) normal to the radial stress, $\tau_{r\theta}$ is the shearing stress in the r, θ-plane, f is the force per unit length and r is the distance from the point of application. Note that we have defined the normal stress to be positive when it produces compression. Fig.2.1. shows the above variables.

Applying the tensor transformation

$$\sigma_x = \sigma_r \cos^2\theta$$

$$\sigma_y = \sigma_r \sin^2\theta$$

we get the stress expression in Cartesian coordinates

$$\sigma_x = \frac{2f}{\pi r}\cos(\alpha - \theta)\cos^2\theta \qquad (2.1a)$$

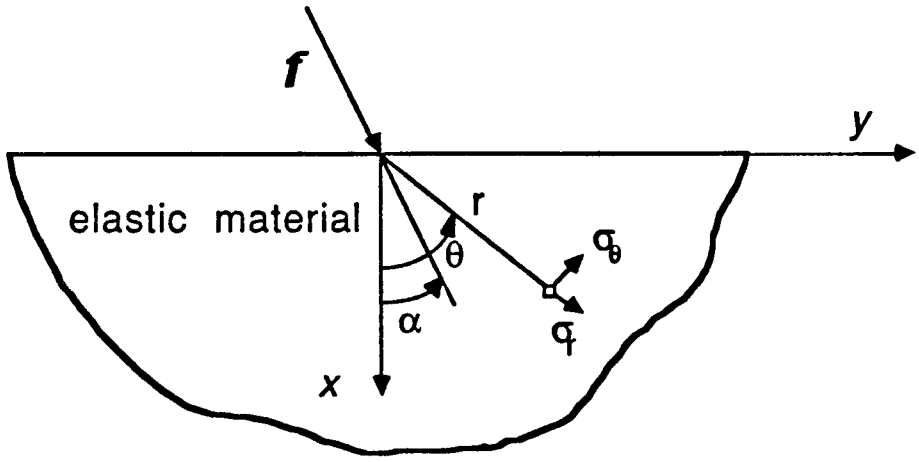

Fig.2.1. Line force on elastic half-plane

$$\sigma_y = \frac{2f}{\pi r} cos(\alpha - \theta) sin^2\theta \tag{2.1b}$$

where $r = \sqrt{x^2 + y^2}$, $cos\theta = x/r$, $sin\theta = y/r$. By decomposing f into vertical component, f_v , and tangential component, f_t , we have

$$sin(\alpha) = \frac{f_t}{f} \tag{2.2a}$$

$$cos(\alpha) = \frac{f_v}{f} \tag{2.2b}$$

Then Eq.(2.1) can be expressed as

$$\sigma_x = \frac{2x^2}{\pi(x^2 + y^2)^2}(xf_v + yf_t) \tag{2.3a}$$

$$\sigma_y = \frac{2y^2}{\pi(x^2 + y^2)^2}(xf_v + yf_t) \tag{2.3b}$$

Applying the principle of superposition, we have, for a load distributed along the y-axis,

$$\sigma_x(x,y) = \int_{-\infty}^{\infty} [K_{x1}^{stress}(x,y-z)f_v(z) + K_{x2}^{stress}(x,y-z)f_t(z)]dz \qquad (2.4)$$

where

$$K_{x1}^{stress}(x,y) = \frac{2x^3}{\pi(x^2+y^2)^2}$$

$$K_{x2}^{stress}(x,y) = \frac{2x^2y}{\pi(x^2+y^2)^2}$$

and

$$\sigma_y(x,y) = \int_{-\infty}^{\infty} [K_{y1}^{stress}(x,y-z)f_v(z) + K_{y2}^{stress}(x,y-z)f_t(z)]dz \qquad (2.5)$$

where

$$K_{y1}^{stress}(x,y) = \frac{2y^2x}{\pi(x^2+y^2)^2}$$

$$K_{y2}^{stress}(x,y) = \frac{2y^3}{\pi(x^2+y^2)^2}$$

for $y \in \mathrm{R}$ and $x \in (0,\infty)$. $f_v(y)$ and $f_t(y)$ are the surface stress distributions in x and y direction, respectively. Fig.2.2a shows the $K_{x1}^{stress}(x,y)$ and $K_{x2}^{stress}(x,y)$ at $x = 1.5$. Fig.2.2b shows the $K_{y1}^{stress}(x,y)$ and $K_{y2}^{stress}(x,y)$ at $x = 1.5$.

2.2 The Expression of Strain due to Surface Contact

Since many pressure sensors have outputs based on the strain of the sensor, which is the fractional change in the linear dimensions of a small cubic volume element, e.g. electric-resistance strain gauges, we need to find the relations between the components of stresses and the components of the strains. By Hooke's Law in the theory of elasticity, we have

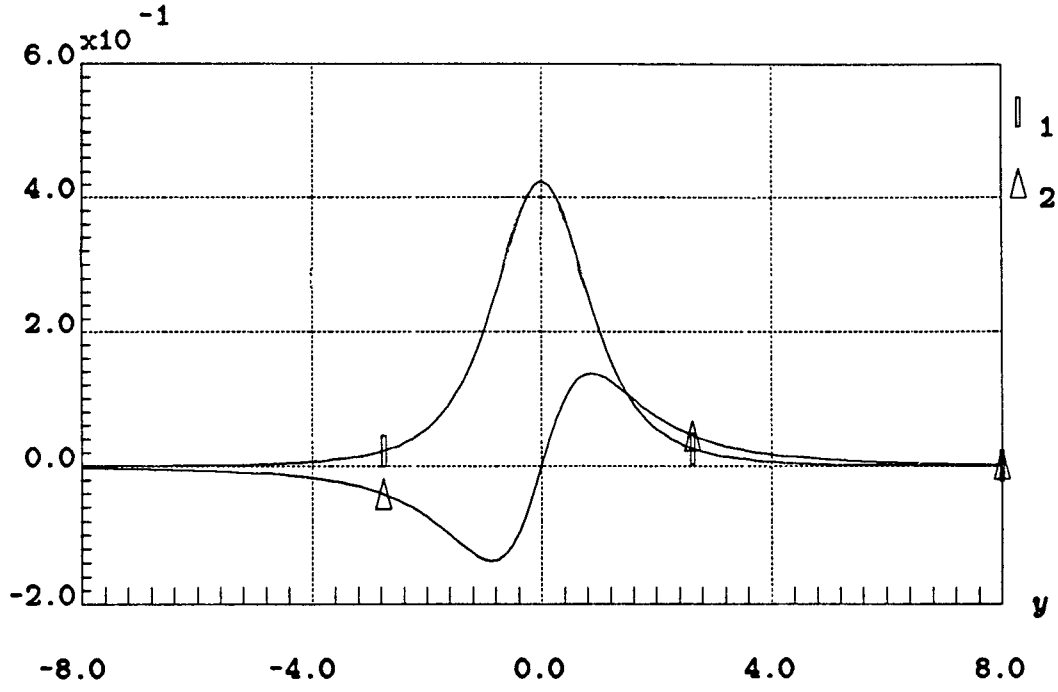

Fig.2.2a 1. $K_{x1}^{stress}(x,y)$ and 2. $K_{x2}^{stress}(x,y)$ at $x = 1.5$

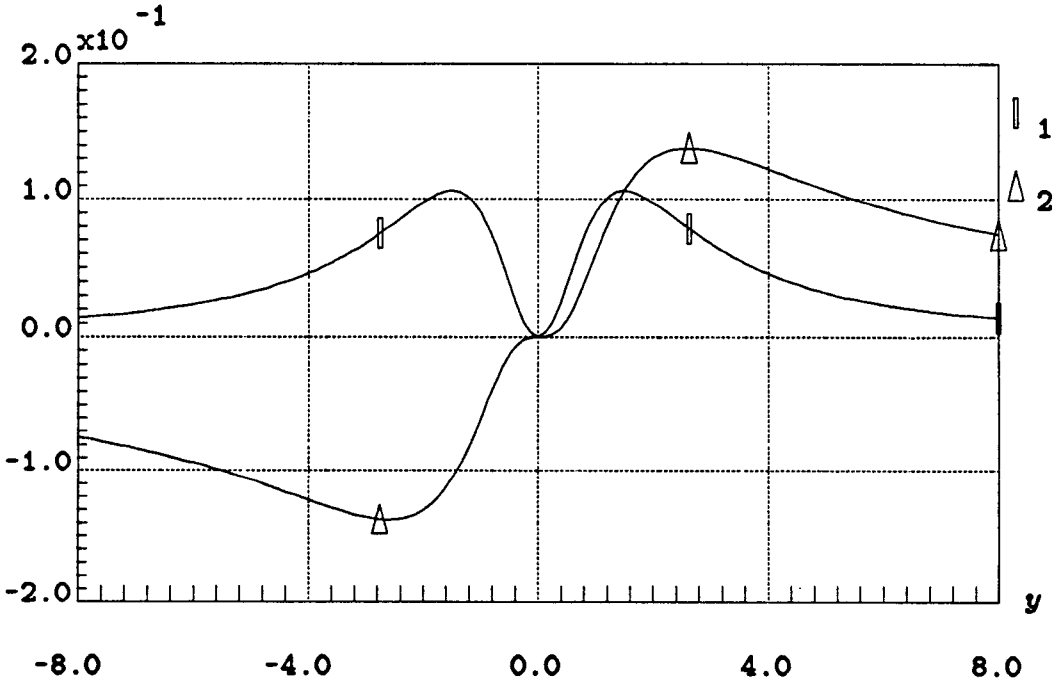

Fig.2.2b 1. $K_{y1}^{stress}(x,y)$ and 2. $K_{y2}^{stress}(x,y)$ at $x = 1.5$

$$\epsilon_x = \frac{1}{E}[\sigma_x - \nu(\sigma_y + \sigma_z)]$$

$$\epsilon_y = \frac{1}{E}[\sigma_y - \nu(\sigma_z + \sigma_x)] \tag{2.6}$$

$$\epsilon_z = \frac{1}{E}[\sigma_z - \nu(\sigma_x + \sigma_y)]$$

where E is the modulus of elasticity, ν is Poisson's ratio, ϵ_x ϵ_y and ϵ_z are the components of the strain along x, y, z directions , respectively.

Since we have assumed in the beginning of this chapter that the dimension of the contact area is infinitely large in z direction, the plane strain assumption can be applied. This assumption states that, for a line force of infinite extent on an elastic half-space, the strain in the direction of the line, ϵ_z, must be zero by symmetry. Then Eq.(2.6) becomes

$$\epsilon_x = \frac{1}{E}[(1-\nu^2)\sigma_x - \nu(\nu+1)\sigma_y] \tag{2.7}$$

$$\epsilon_y = \frac{1}{E}[(1-\nu^2)\sigma_y - \nu(\nu+1)\sigma_x]$$

From Eq.(2.7), we can get the expressions of σ_x and σ_y in terms of ϵ_x and ϵ_y (assuming $\nu \neq 0.5$)

$$\sigma_x = \lambda[(1-\nu)\epsilon_x + \nu\epsilon_y] \tag{2.8a}$$

$$\sigma_y = \lambda[(1-\nu)\epsilon_y + \nu\epsilon_x] \tag{2.8b}$$

where

$$\lambda = \frac{E}{(1+\nu)(1-2\nu)}$$

It should be note that if ν=0.5, from Eq.(2.7), $\epsilon_x = -\epsilon_y = \frac{3}{4E}(\sigma_x - \sigma_y)$. That means that ϵ_x and ϵ_y are not independent. So, we will have insufficient information to determine σ_x and σ_y from ϵ_x and ϵ_y.

Again, using the principle of superposition for general contact, we have

$$\epsilon_x(x,y) = \int_{-\infty}^{\infty} [K_{x1}^{strain}(x,y-z)f_v(z) + K_{x2}^{strain}(x,y-z)f_t(z)]dz \qquad (2.9)$$

where

$$K_{x1}^{strain}(x,y) = \frac{2x}{\pi E(x^2+y^2)^2}[(1-\nu^2)x^2 - \nu(\nu+1)y^2)]$$

$$K_{x2}^{strain}(x,y) = \frac{2y}{\pi E(x^2+y^2)^2}[(1-\nu^2)x^2 - \nu(\nu+1)y^2)]$$

and

$$\epsilon_y(x,y) = \int_{-\infty}^{\infty} [K_{y1}^{strain}(x,y-z)f_v(z) + K_{y2}^{strain}(x,y-z)f_t(z)]dz \qquad (2.10)$$

where

$$K_{y1}^{strain}(x,y) = \frac{2x}{\pi E(x^2+y^2)^2}[(1-\nu^2)y^2 - \nu(\nu+1)x^2)]$$

$$K_{y2}^{strain}(x,y) = \frac{2y}{\pi E(x^2+y^2)^2}[(1-\nu^2)y^2 - \nu(\nu+1)x^2)]$$

for $y \in$ R and $x \in (0,\infty)$. Fig.2.3a shows the $K_{x1}^{strain}(x,y)$ and $K_{x2}^{strain}(x,y)$ at $x = 1.5$. Fig.2.3b shows the $K_{y1}^{strain}(x,y)$ and $K_{y2}^{strain}(x,y)$ at $x = 1.5$. In both of these figures, $\nu = 0.45$.

2.3 Some Assumptions

For the sake of convenience, we write Eq.(2.4), (2.5), (2,9) and (2.10) in the general form as

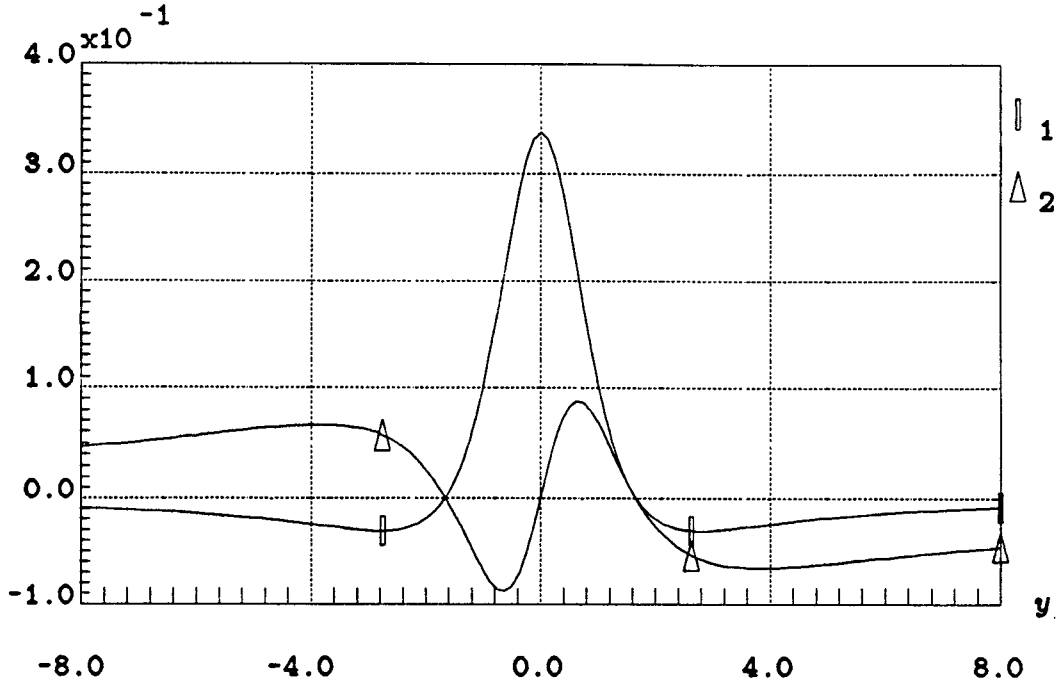

Fig.2.3a 1. $K_{x1}^{strain}(x,y)$ and 2. $K_{x2}^{strain}(x,y)$ at $x = 1.5$

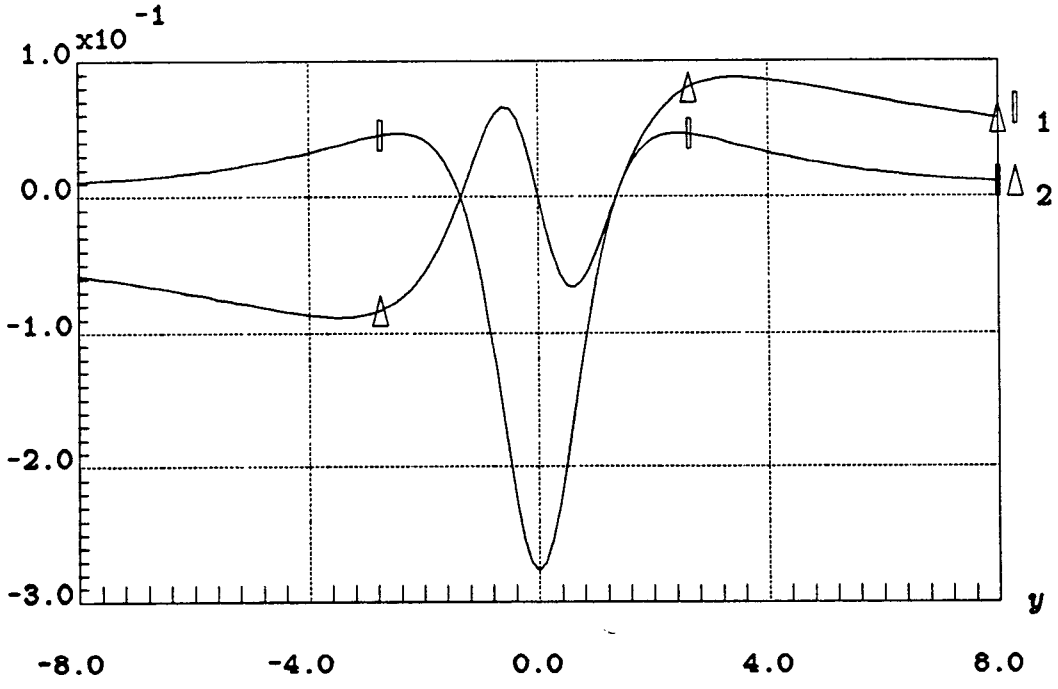

Fig.2.3b 1. $K_{y1}^{strain}(x,y)$ and 2. $K_{y2}^{strain}(x,y)$ at $x = 1.5$

$$g(y) = \int_{-\infty}^{\infty} [K_1(y-z)f_v(z) + K_2(y-z)f_t(z)]dz \tag{2.11}$$

where $y \in R$. We will indicate that K_1, K_2 and g are in the form of stress or strain and in x or y direction when it is necessary. In Eq.(2.11), there is no x dependence since we assume that the array of tactile sensors is usually mounted on a horizontal plane beneath the surface of elastic material. Thus, x in Eq.(2.11) is a constant which expresses the depth of the sensors from the surface.

Eq.(2.11) expresses the relationship between surface stress profile and the strain or stress distribution beneath the surface, in which $g(y)$ is the known function obtained by tactile sensors, $f_v(y)$ and $f_t(y)$ are unknown functions. This equation is an integral equation of first kind with two unknown functions. It should be mentioned that Fearing and Hollerbach (1985) derived the elastic model with the form as

$$g(y) = \int_{-\infty}^{\infty} K[y-z, \alpha(z)]f(z)dz$$

where $\alpha(z)$ and $f(z)$ are unknown. This equation is not easy to be solved since $g(y)$ is not the linear functional of $\alpha(z)$.

In the next two chapters, we shall study numerical approaches to solve the equation. In the beginning of each of them, we shall first study Eq.(2.11) without considering tangential components of surface force, i.e.

$$g(y) = \int_{-\infty}^{\infty} K_1(y-z)f_v(z)dz \tag{2.12}$$

And then, under some conditions, we shall explore the approaches to solve Eq.(2.11).

Moreover, we make the following assumptions:

The assumption about $f(y)$: We assume that $f_v(y)$ is produced by the strip contact, i.e. it satisfies

$$f_v(y) = \begin{cases} f_1(y), & \text{if } y \in [a_1, a_2]; \\ 0, & \text{otherwise,} \end{cases}$$

where $f_1(y)$ is a continuous function defined on $[a_1, a_2]$, $f_1(y) > 0$ for $y \in (a_1, a_2)$ and $f_1(y) \geq 0$ at $y = a_1$ and $y = a_2$, for some finite a_1 and a_2. Moreover, we will assume that $\mid a_i \mid < A/2$, $i = 1, 2$, where A is the half width of surface of the finger. We make this assumption because, even for a very narrow force profile, a broad distribution of stress and strain will be produced . This is illustrated by Fig.2.2 and Fig.2.3 which show respectively the distribution of stress and strain due to line contact when we let one of f_v and f_t be a unit impulse function and another be zero. In other words, for a strip contact, we need the observations which distribute more broadly than the width of the strip to obtain the surface force profile. $f_t(y)$ is produced by static friction.

The assumption about $g(y)$: We assume that, in the sense of the norm we shall use, the observation of $g(y)$ is very close to the true value which is produced by Eq.(2.11) and is without noise corruption. In Tikhonov (1977) the discussions of the problems with the noise have been given. One of the ideas is to suppress the influence of the components of the high frequency of noise. So, we also can assume that the observations have been processed by a suitable low-pass filter.

CHAPTER

THREE

THE DFT APPROACH FOR THE INVERSE PROBLEM

In this chapter, we shall apply the method based on discrete Fourier transformation(DFT) to solve the inverse problem approximately. We assume that the observation, $g(y)$, is the interior strain or stress in x direction. Thus, we shall study Eq.(2.4) and (2.9). Meanwhile, we suppose $\nu = 0.5$.

In section 3.1, we shall briefly study the DFT method to solve Eq.(2.12). In section 3.2, based on the result in section 3.1, we shall derive the algorithm to solve Eq.(2.11) approximately. In section 3.3, some examples will be given.

3.1 Surface Force Profile without Tangential Component

Rewrite Eq.(2.11) as follows

$$g(y) = \int_{-\infty}^{\infty} K_1(y-z) f_v(z) dz \qquad y \in R \tag{3.1}$$

This integral equation is of convolution type, in which $g(y)$ is the observation obtained by sensors, $f_v(y)$ is an unknown function, $K_1(y)$ is known function, usually called *the kernel.*

It is known that the Fourier transform of the convolution of K_1 and f_v equals the normal multiplication of Fourier transform of K_1 and f_v if

$$\int_{-\infty}^{\infty} \mid K_1(y) \mid dy < \infty$$

and

$$\int_{-\infty}^{\infty} \mid f_v(y) \mid dy < \infty$$

That is,

$$\hat{K}_1(\omega)\hat{f}_v(\omega) = \hat{g}(\omega) \tag{3.2}$$

where $\hat{K}_1(\omega), \hat{f}_v(\omega)$ and $\hat{g}(\omega)$ are Fourier transforms of K_1, f_v and g, respectively. By the assumption about f_v and $K_{x1}^{stress}, K_{x1}^{strain}$ given in Chapter 2, one can check that the conditions of (3.2) are satisfied. It is clear that if (a). $\hat{K}_1(\omega) \neq 0, \forall |\omega| < \infty$, and (b). $\hat{g}(\omega)/\hat{K}_1(\omega) \in L_1(-\infty, \infty)$, the Eq.(3.1) can be solved simply as

$$f_v(y) = \mathcal{F}^{-1}(\frac{\hat{g}(\omega)}{\hat{K}_1(\omega)}) \qquad y \in R \tag{3.3}$$

where $\mathcal{F}^{-1}$ is the operator of the inverse Fourier transformation .

Physically, it is difficult to make the condition (b) satisfied because of the existence of the noise. Tikhonov (1977) gave some approaches to solve this problem. Since our purpose is to solve Eq.(2.11), by the assumption about $g(y)$ given in Chapter 2, we assume condition (b) is satisfied. On the other hand, it is easy to check that the Fourier transforms of K_{x1}^{stress} and K_{x1}^{strain} given in Eq.(2.4) and Eq.(2.9) are

$$\hat{K}_{x1}^{stress}(\omega) = e^{-x|\omega|}(1 + x|\omega|) \quad \omega \in R$$

and

$$\hat{K}_{x1}^{strain}(\omega) = 1.5x|\omega|e^{-x|\omega|} \quad \omega \in R$$

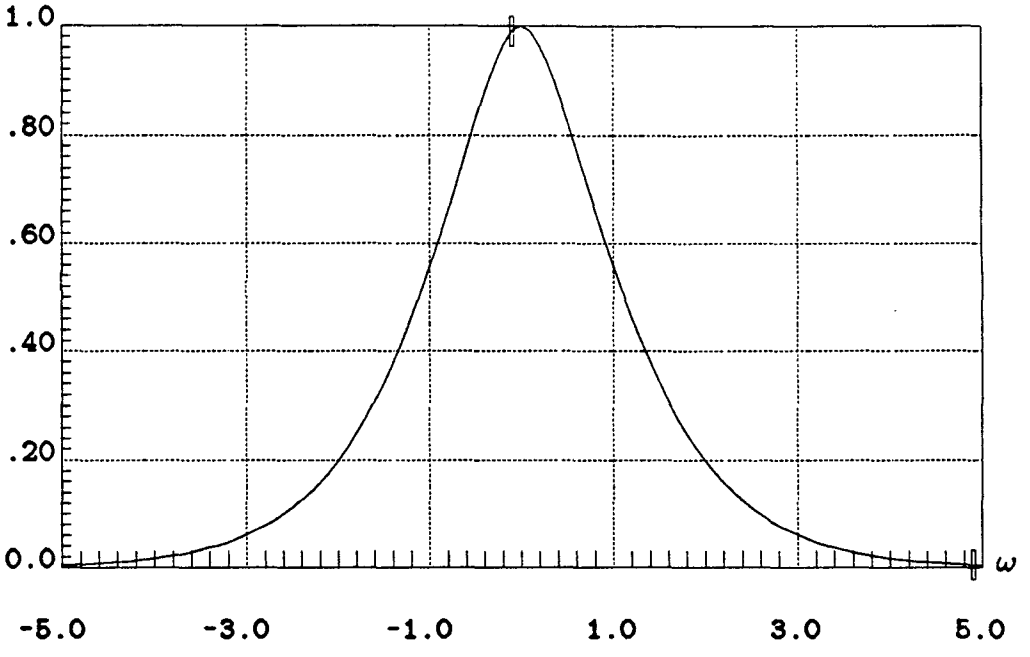

Fig.3.1. The Fourier transform of K_{x1}^{stress} at $x = 1.5$.

It is clear that if the distribution of stress can be obtained directly or indirectly by sensors, the condition (a) is satisfied (see Fig.3.1).

If we have to use the distribution of strain, the condition (a) can not be satisfied since $\hat{K}_{x1}^{strain}(0) = 0$, (see Fig.3.2). We will see that this problem can be solved when the observation, $g(y)$, is truncated and DFT is applied.

Physically, the continuous expression of $g(y)$ can not be obtained directly, but only the discrete data of $g(y)$. So, we are forced to apply the discrete Fourier transform to solve the inverse problem approximately.

The discretization of Eq. (3.1) is

$$g(y_n) = \sum_{i=-\infty}^{\infty} K_1(y_n - y_i) f_v(y_i) \triangle y_i \qquad n = 0, \pm 1, \pm 2, \ldots \tag{3.4}$$

where $\triangle y_i = y_{i+1} - y_i$ called *sampling period.* If we let $\triangle y_i$ be identical for all i, denoted by $\triangle$, and denote $g(y_n)$ by $g(n)$, $K_1(y_n - y_i)\triangle y_i$ by $K_1(n - i)$ and

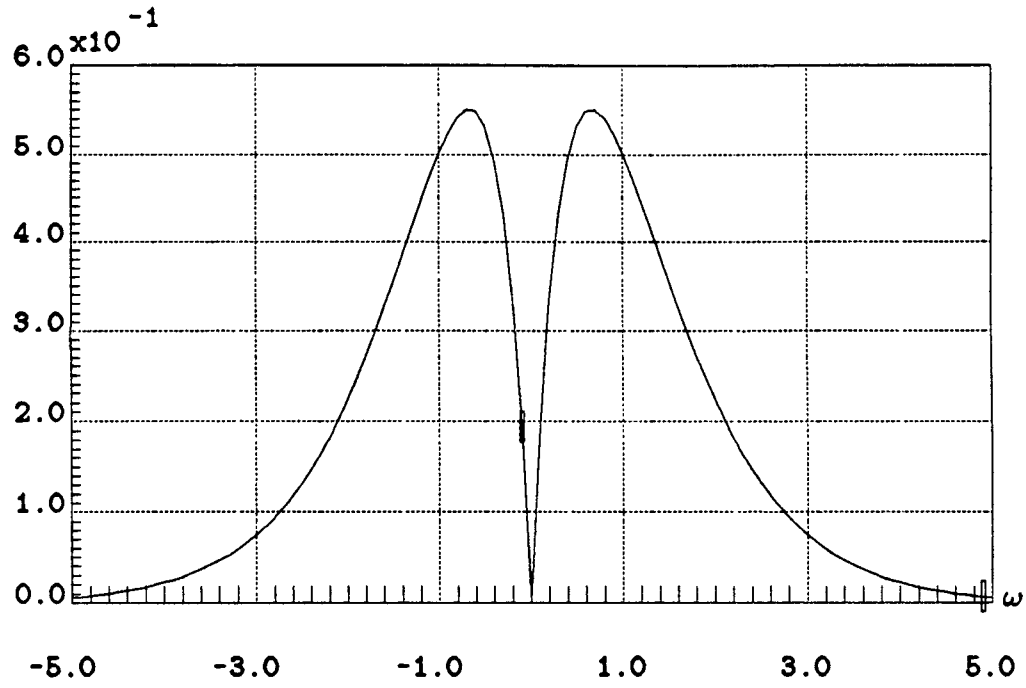

Fig.3.2 The Fourier transform of K_{x1}^{strain} at $x = 1.5$.

$f_v(y_i)$ by $f_v(i)$, then Eq.(3.4) can be written as

$$g(n) = \sum_{i=-\infty}^{\infty} K_1(n-i) f_v(i) \qquad n = 0, \pm 1, \pm 2, \ldots \tag{3.5}$$

This is the discrete convolution equation. It should be noted that, physically, it is impossible to get the data of observation, $g(n)$, everywhere. We have to cut off $g(n)$, at $n = -N$ and N,where $N\Delta = A$. Due to the properties of $K_{1x}^{stress}(y)$ and $K_{1x}^{strain}(y)$ and the assumption about $f_v(y)$, if A is large enough, $g(N)$ should be very small. Then, we can replace Eq.(3.5) by

$$g(n) = \sum_{i=-N}^{N} K_1(n-i) f_v(i) \qquad n = 0, \pm 1, \pm 2, \ldots, \pm N \tag{3.6}$$

It is known that the discrete Fourier transform of convolution of $K_1(i)$ and $f_v(i)$ is the normal multiplication of DFT of them. So, we have

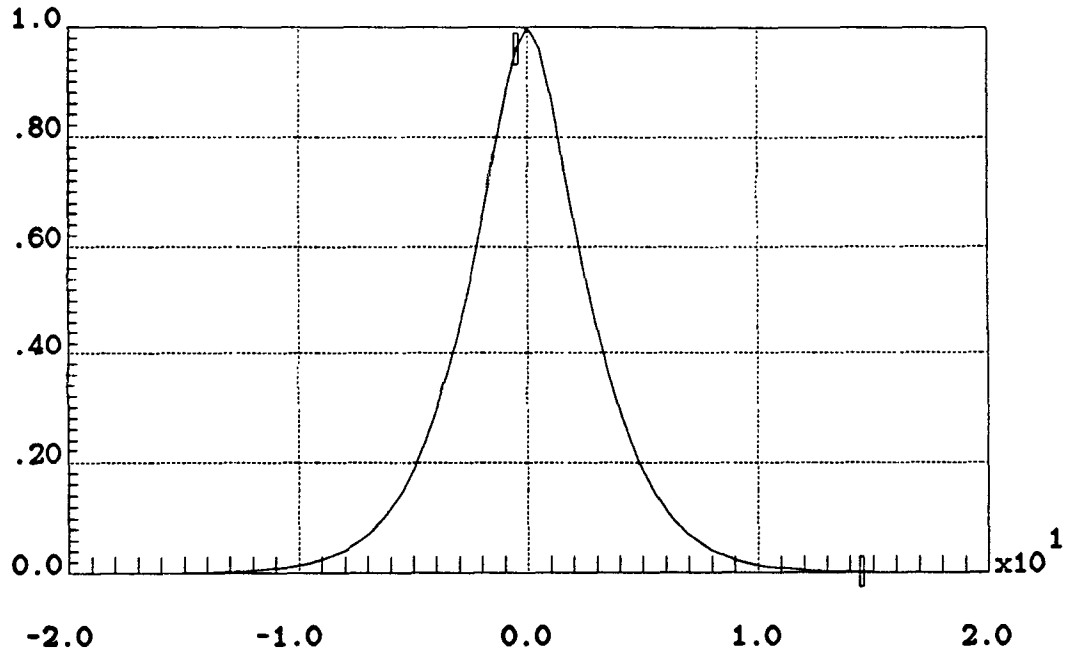

Fig.3.3 The DFT of K_{z1}^{stress}

$$\hat{g}(k) = \hat{K}_1(k)\hat{f}_v(k) \qquad k = 0, \pm 1, \pm 2, ..., \pm N \tag{3.7}$$

where $\hat{g}(k) = \sum_{i=-N}^{N} g(i)e^{-j2\pi ik/2N+1}$, $j = \sqrt{-1}$, $k = 0, \pm 1, \ldots, \pm N$ is the DFT of $g(i)$, and similarly to $\hat{K}_1(k)$ and $\hat{f}_v(k)$. Fig.3.3 and Fig.3.4 give the DFT of K_1^{stress} and K_1^{strain}.

From the theory of digital signal processing (Chen,1979), we know that, for given function $K(y)$, the discrete Fourier transform of it, say $\hat{K}(k)$, is the evaluation of z-transformation of this function, say $\hat{K}(z)$, on the unit circle of the z-plane. In other words,

$$\hat{K}(k) = \hat{K}(z)|_{z=e^{j\omega_k \Delta}}$$

for $\omega_k = \frac{2k\pi}{(2N+1)\Delta}$, $k = 0, \pm 1, \pm 2, ..., \pm N$. We also know that the z-transformation evaluated on the unit circle and Fourier transformation are related by

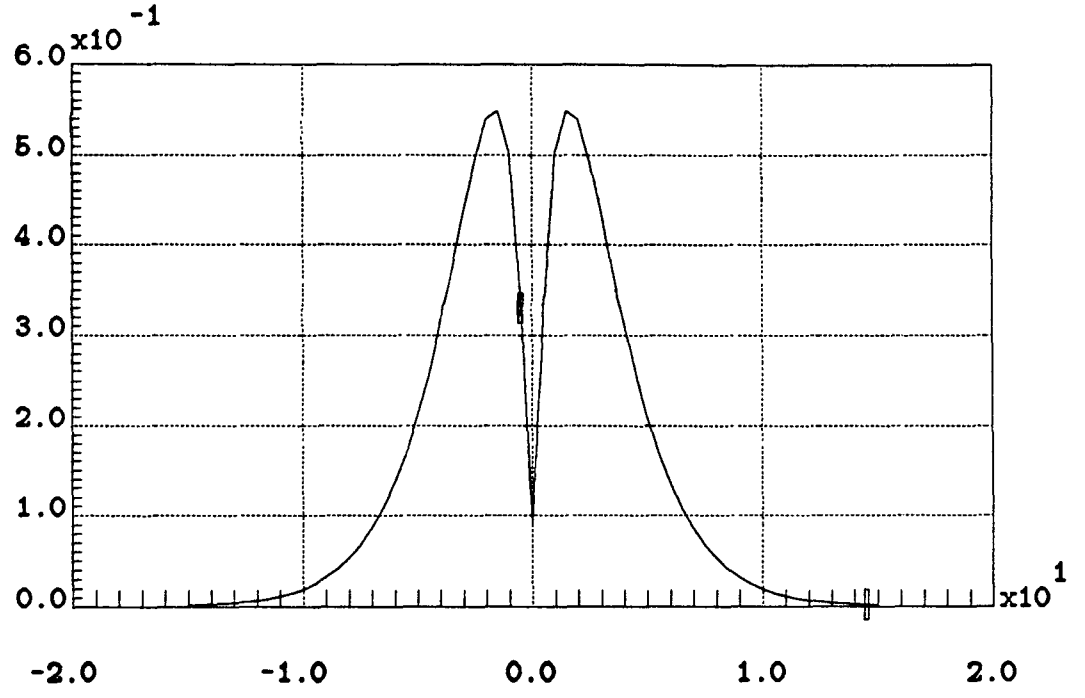

Fig.3.4 The DFT of K_{x1}^{strain}

$$\hat{K}(e^{j\omega\Delta}) = [\sum_n \hat{K}(\omega + n\omega_s)]/\Delta$$

where $\omega_s = 2\pi/\Delta$. From this formula, we can say that, if the Fourier transform of $K(y)$ is very small for $|\omega| > \omega_s/2$,

$$\hat{K}(k) = \hat{K}(z)|_{z=e^{j\omega_k\Delta}} \simeq \frac{1}{\Delta}\hat{K}(\omega)|_{\omega=\omega_k}$$

where $\omega_k = \frac{2k\pi}{(2N+1)\Delta}$, $k = 0, \pm 1, \pm 2, ..., \pm N$.

Comparing Fig.3.1 and Fig.3.2 with Fig.3.3 and Fig.3.4, we find $K_{x1}^{stress}(y)$ and $K_{x1}^{strain}(y)$ are satisfied the above condition and result. It should be noted that for K_{x1}^{strain}, they are different at 0. The reason is that our function is truncated at $|y| = A$ and $K_1(A) \neq 0$, even it is very small. This is just right for us to apply the DFT to solve the inverse problem.

Applying inverse discrete Fourier transform, the unknown function, $f_v(k)$, is

$$f_v(k) = \frac{1}{2N+1} \sum_{r=-N}^{N} (\frac{\hat{g}(r)}{\hat{K}_1(r)}) e^{j2\pi rk/2N+1} \qquad k = 0, \pm 1, ... \pm N \tag{3.8}$$

In section 3.3, by example, we will find that the reconstructed function produced by Eq.(3.8) has very good accuracy with respect to the designed one. We will also discuss the effect of truncation and the choice of K_1.

3.2 Surface Force Profile with Tangential Component

In this section, the relation between vertical component of surface stress, f_v, and tangential one, f_t, is based on the knowledge of the characteristic of the friction on the contact surface. In order to avoid slipping during grasping, we are interested in the tangential force on the average, instead of at every point (see Chapter 6). It is assumed that the relation of $f_t(y)$ and $f_v(y)$ at the boundary of cone of friction is estimated by

$$\int_{a_1}^{a_2} f_t(y)dy = \mu \int_{a_1}^{a_2} f_v(y)dy,$$

where μ is the coefficient of static friction. Moreover, we assume that $a \stackrel{\text{def}}{=} -a_1 = a_2$ since we will need to determine the boundary of the load from $g(y)$. By the Mean Value Theorem, we have

$$c = \frac{\mu}{2a} \int_{-a}^{a} f_v(y)dy \tag{3.9}$$

where c is a constant. As an approximation, we will substitute this constant for $f_t(y)$ on $[-a, a]$, i.e.

$$f_t(y) = \begin{cases} c, & \text{if } y \in [-a, a]; \\ 0, & \text{otherwise,} \end{cases}$$

Under above assumptions, Eq.(2.11) becomes

$$g(y) = \int_{-\infty}^{\infty} [K_1(y-z) f_v(z) + \frac{\mu}{2a} K_2(y-z) \int_{-\infty}^{\infty} f_v(u) du] dz \tag{3.10}$$

Next, we will discuss how to solve Eq.(3.10) numerically.

By discretizing Eq.(3.10) and truncating the observation, we have

$$g(n) = \sum_{i=-N}^{N} K_1(n-i) f_v(i) + \frac{\mu}{2M} (\sum_{i=-N}^{N} u(i) K_2(n-i)) (\sum_{k=-N}^{N} f_v(k))$$

$$n = 0, \pm 1, \ldots, \pm N \tag{3.11}$$

in which M is taken such that $2a = 2M\triangle$, and $u(i)$ is defined as

$$u(i) = \begin{cases} 1, & \text{for } i : i\triangle \in [-a, a]; \\ 0, & \text{otherwise.} \end{cases}$$

Applying DFT to Eq.(3.11), we have

$$\sum_{n=-N}^{N} g(n) w^{nr} = (\sum_{n=-N}^{N} K_1(n) w^{nr}) (\sum_{n=-N}^{N} f_v(n) w^{nr})$$

$$+ \frac{\mu}{2M} (\sum_{n=-N}^{N} f_v(n)) (\sum_{n=-N}^{N} K_2(n) w^{nr}) (\sum_{n=-N}^{N} u(n) w^{nr})$$

$$r = 0, \pm 1, ..., \pm N$$

where $w = e^{-j2\pi/2N+1}, j = \sqrt{-1}$. When $r = 0$,

$$\sum_{n=-N}^{N} g(n) = (\sum_{n=-N}^{N} K_1(n)) (\sum_{n=-N}^{N} f_v(n))$$

$$+ \frac{\mu(2M+1)}{2M} (\sum_{n=-N}^{N} K_2(n)) (\sum_{n=-N}^{N} f_v(n)) \tag{3.12}$$

Since $K_2(y)$ is an odd function, we have

$$\sum_{n=-N}^{N} K_2(n) = 0$$

Therefore, Eq.(3.12) becomes

$$F \stackrel{\text{def}}{=} \sum_{n=-N}^{N} f_v(n) = (\sum_{n=-N}^{N} g(n))(\sum_{n=-N}^{N} K_1(n))^{-1}$$

Discretizing Eq.(3.9), we have

$$c = \frac{\mu}{2M} F \tag{3.13}$$

Returning to Eq.(3.11), we have

$$g(n) - c \sum_{i=-M}^{M} K_2(n-i) = \sum_{i=-N}^{N} K_1(n-i) f_v(i) \qquad n = 0, \pm 1, ..., \pm N \tag{3.14}$$

Denoting left hand side of previous equation as $G(n)$, Eq.(3.14) becomes

$$G(n) = \sum_{i=-N}^{N} K_1(n-i) f_v(i) \qquad n = 0, \pm 1, ... \pm N \tag{3.15}$$

This is the equation we have solved in above section. However, the problem of this section has not been solved since we do not know M yet. As we have assumed before, $f_v(y)$ and $f_t(y)$ have symmetric support, $[-a, a]$. And we will see in the next section that the algorithm in section 3.1 has a very good accuracy. By these properties, we can find M. The method is shown as follows.

We have known that

$$g(y) = \int_{-\infty}^{\infty} K_1(y-z) f_v(z) + K_2(y-z) f_t(z) dz$$

Then,

$$g(-y) = \int_{-\infty}^{\infty} K_1(-y-z) f_v(z) + K_2(-y-z) f_t(z) dz$$

By changing the integral variable and utilizing the odd and even property of $K_1(y)$ and $K_2(y)$, we have

$$g(-y) = \int_{-\infty}^{\infty} K_1(y-z) f_v(-z) - K_2(y-z) f_t(-z) dz$$

Since we assumed that $f_t(y)$ is a constant, taking the average of $g(y)$ and $g(-y)$, we have

$$\tilde{g}(y) = \int_{-\infty}^{\infty} K_1(y-z) \tilde{f}_v(z) dz \tag{3.16}$$

where $\tilde{g}(y) = [g(y) + g(-y)]/2$, $\tilde{f}_v(y) = [f_v(y) + f_v(-y)]/2$.

By the assumption of $f_v(y)$, $\tilde{f}_v(y)$ still have a symmetric support, $[-a, a]$. Therefore, applying the DFT to Eq.(3.16), we can find M by the algorithm in section 3.1.

3.3 Examples

In this section we will give some examples for some special load profiles and compare the results which are obtained from the observations expressed as the distribution of stress and distribution of strain when $\nu = 0.5$.

Some parameters are fixed as follows.

- the depth of the sensors, $x = 1.5$
- the sampling period, $\triangle = 0.5$
- the modulus of elasticity, $E = 1$
- the numbers of elements of sensors, $2N + 1 = 121$

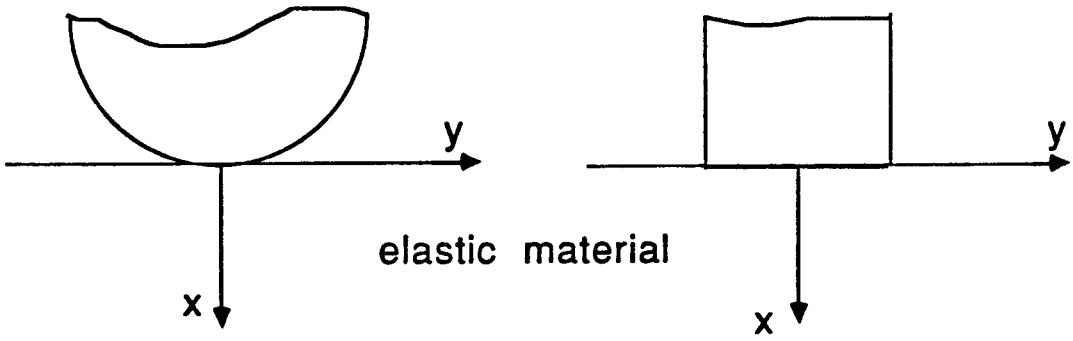

Fig.3.5 The cylindrical and rectangular indentor

In the following examples, $g(y)$ is produced by the discrete form of Eq.(2.4) and Eq.(2.9) directly. To evaluate the reconstructed surface stress, f, with respect to designed one, f^d, we use the absolute error defined as

$$e = \frac{1}{2N+1} \sum_{i=-N}^{N} |f^d(i) - f(i)|. \tag{3.17}$$

We will consider two kinds of rigid load: cylinder and rectangle, as shown in Fig.3.5.

From Conway et al. (1966), for cylinder indenting an elastic half-plane, the surface stress is given by

$$f_v(y) = \begin{cases} \frac{2P}{\pi a^2}\sqrt{a^2 - y^2}, & \text{for } y \in [-a, a]; \\ 0, & \text{otherwise,} \end{cases}$$

where a is the half-width of the contact region and P is the force per length; for rectangular indentor, the stress on the surface is given by

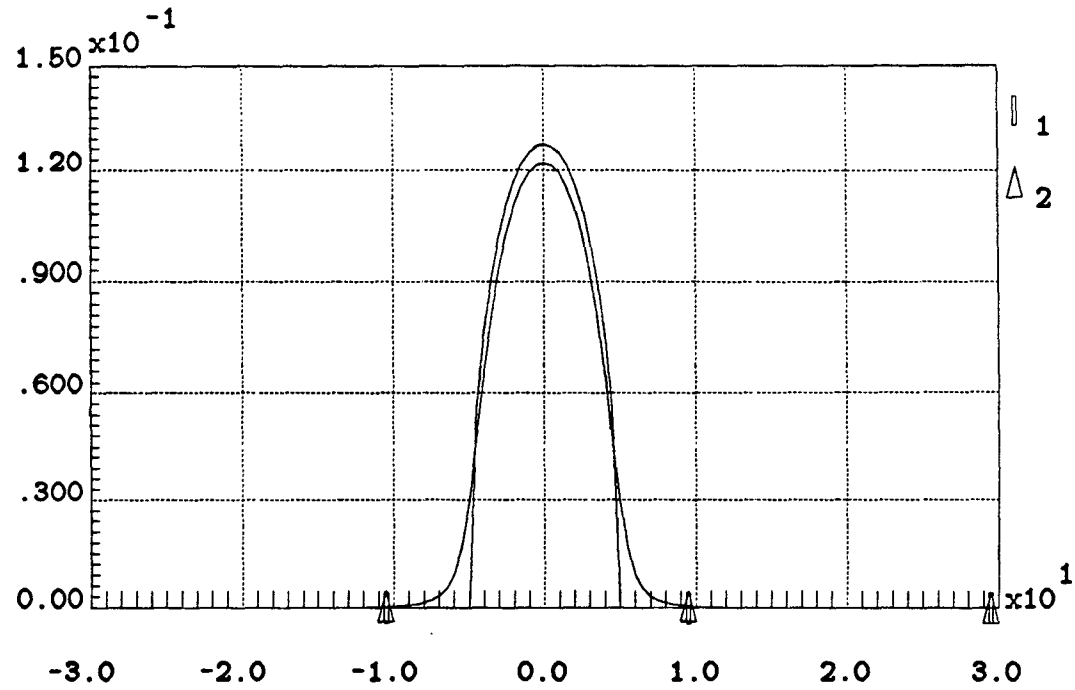

Fig.3.6a 1. the designed surface stress; 2. the stress at $x = 1.5$

$$f_v(y) = \begin{cases} \frac{P}{\pi\sqrt{(a+\epsilon)^2-y^2}}, & \text{for } y \in [-a,a]; \\ 0, & \text{otherwise,} \end{cases}$$

for $\epsilon \ll 1$.

Example 3.1 Cylinder indenting without friction

The distributions of stress and strain at $x = 1.5$ produced by a cylindrical indentor are given in Fig.3.6a and Fig.3.6c, respectively, in which the designed surface stresses are also displayed. By applying Eq.(3.8), Fig.3.6b and Fig.3.6d give the surface stress reconstructed from the observations given in Fig.3.6a and Fig.3.6c, respectively. For comparison, the designed surface stresses are displayed again.

By Eq.(3.17), the errors for these two cases are

$$e^{stress} = 3.93 \times 10^{-6} \quad , e^{strain} = 4.04 \times 10^{-5}$$

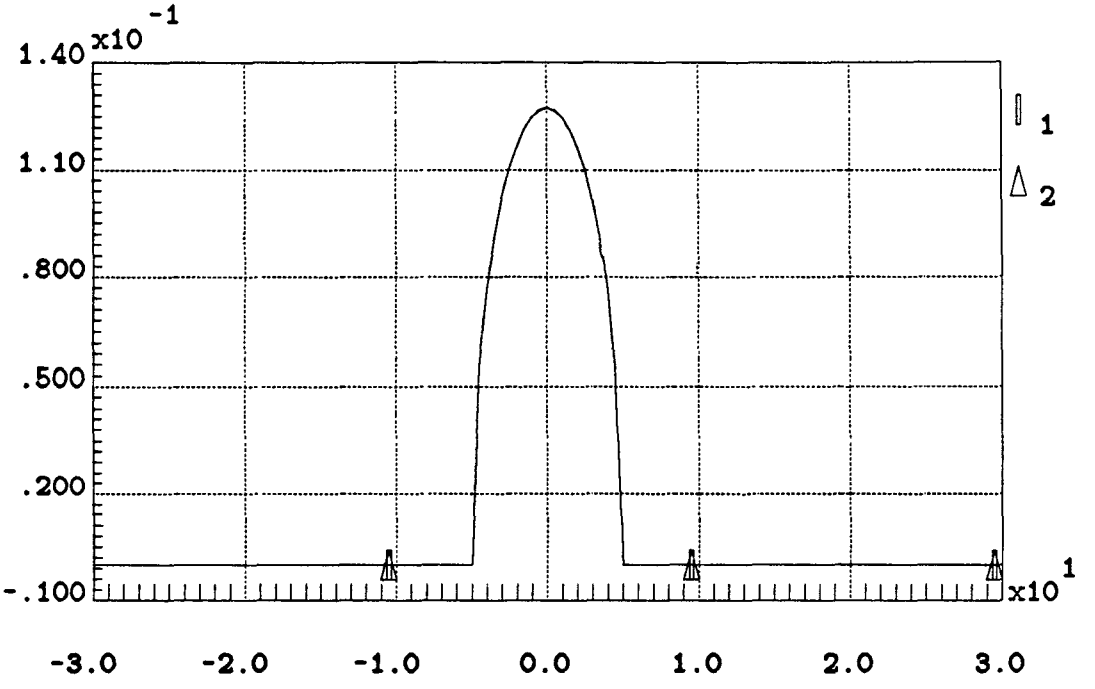

Fig.3.6b 1. the designed surface stress; 2. the reconstructed surface stress

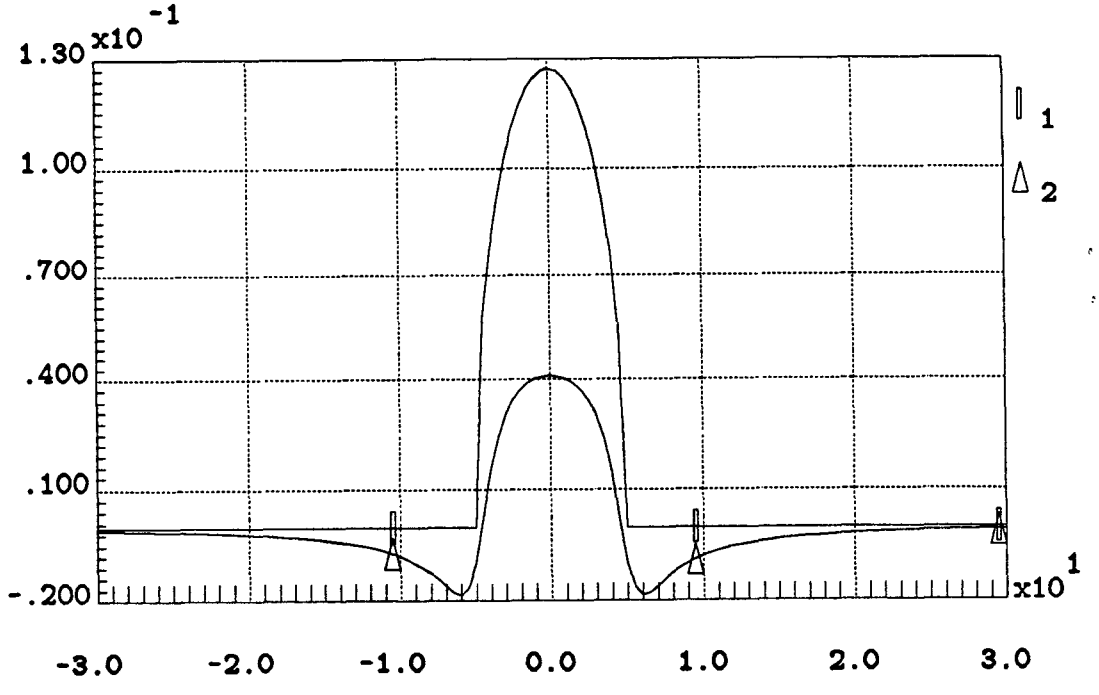

Fig.3.6c 1. the designed surface stress; 2. the strain at $x = 1.5$

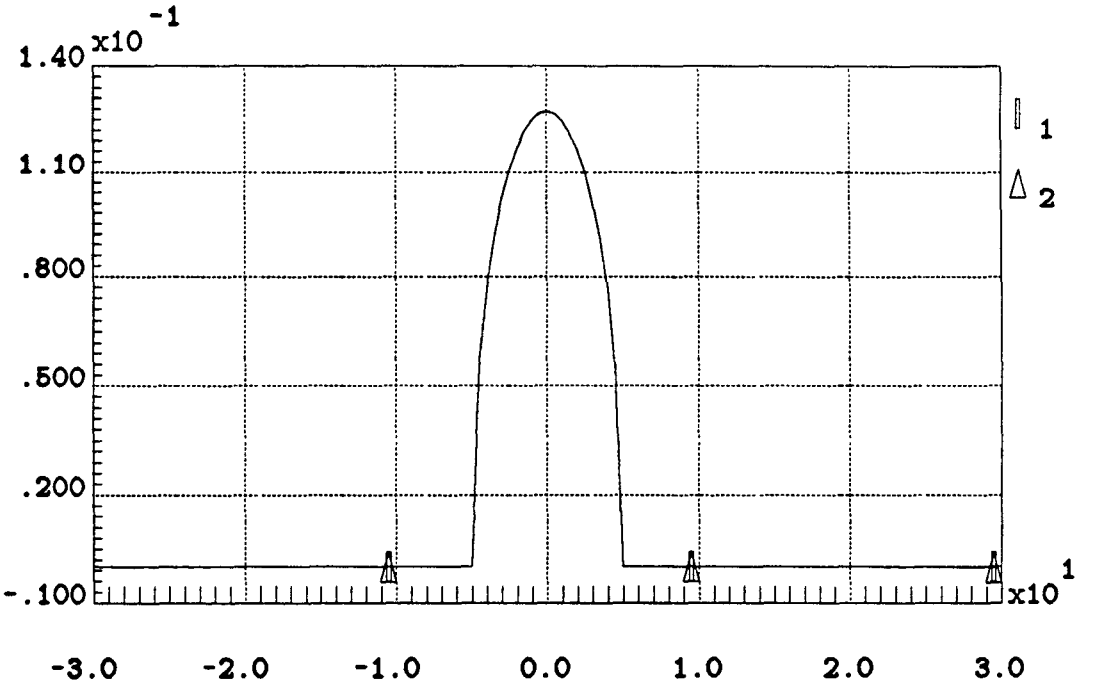

Fig.3.6d 1. the designed surface stress; 2. the reconstructed surface stress

Example 3.2 Rectangular indenting with constant friction

The distributions of stress and strain at $x = 1.5$ produced by cylindrical indentor are given in Fig.3.7a and Fig.3.7c, respectively, in which the designed surface stresses in vertical and tangential direction are also displayed. By applying Eq.(3.13) and (3.14), Fig.3.7b and Fig.3.7d give the surface stresses reconstructed from the observations given in Fig.3.7a and Fig.3.7c, respectively. For comparing, the designed surface stresses are displayed again.

By Eq.(3.17), the errors for these two cases are

$$e_v^{stress} = 6.21 \times 10^{-5}, \quad e_t^{stress} = 1.15 \times 10^{-3}$$

$$e_v^{strain} = 2.95 \times 10^{-3}, \quad e_t^{strain} = 1.45 \times 10^{-3}$$

where the subscripts v and t are expressed for vertical and tangential component, respectively.

From above examples, we find that $e^{strain} > e^{stress}$ for all cases. There are

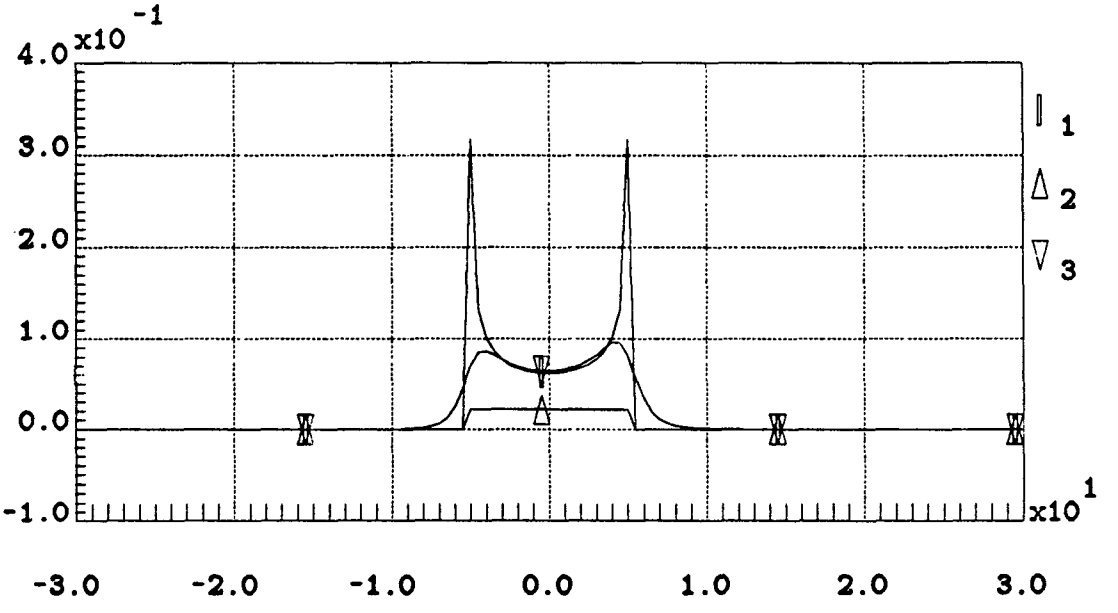

Fig.3.7a 1. the designed vertical surface stress;
2. the designed tangential surface stress;
3. the stress at $x = 1.5$

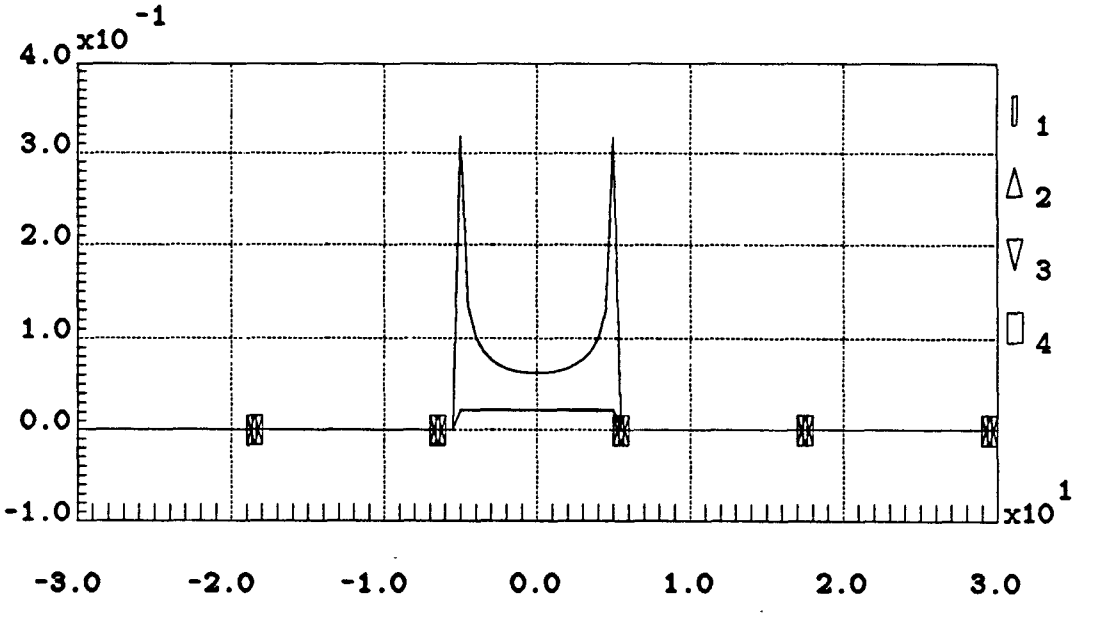

Fig.3.7b 1. the designed vertical surface stress;
2. the reconstructed vertical surface stress;
3. the designed tangential surface stress;
4. the reconstructed tangential surface stress.

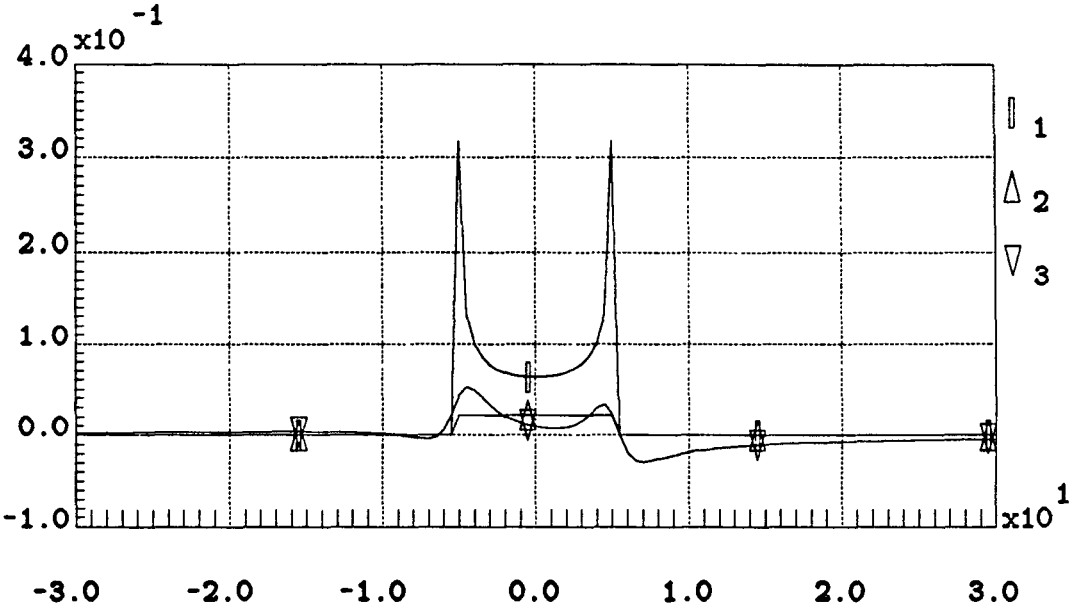

Fig.3.7c 1. the designed vertical surface stress;
2. the designed tangential surface stress;
3. the strain at $x = 1.5$

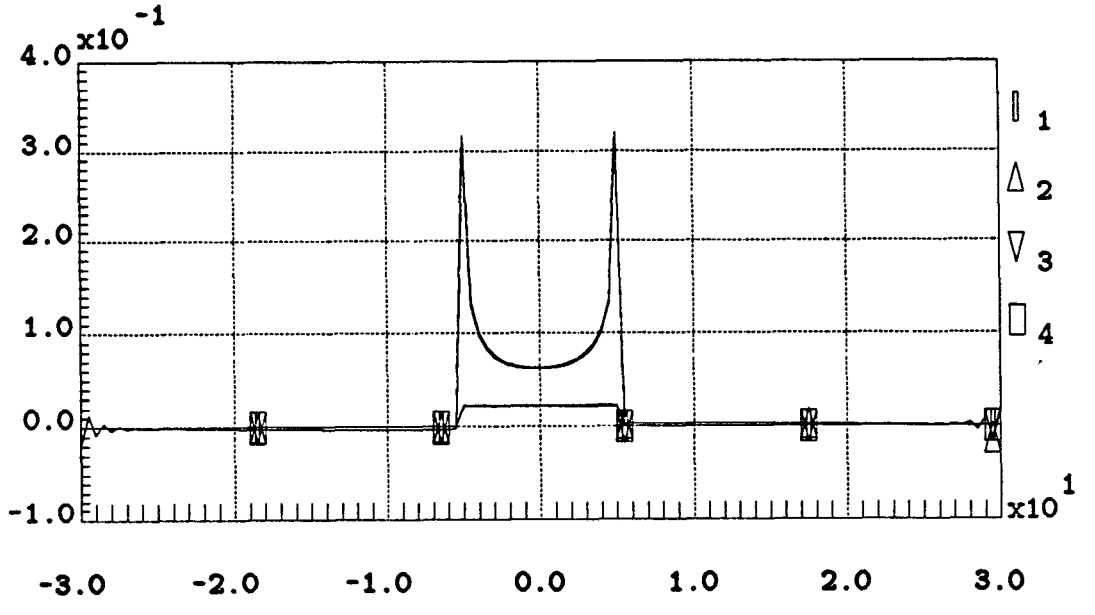

Fig.3.7d 1. the designed vertical surface stress;
2. the reconstructed vertical surface stress;
3. the designed tangential surface stress;
4. the reconstructed tangential surface stress.

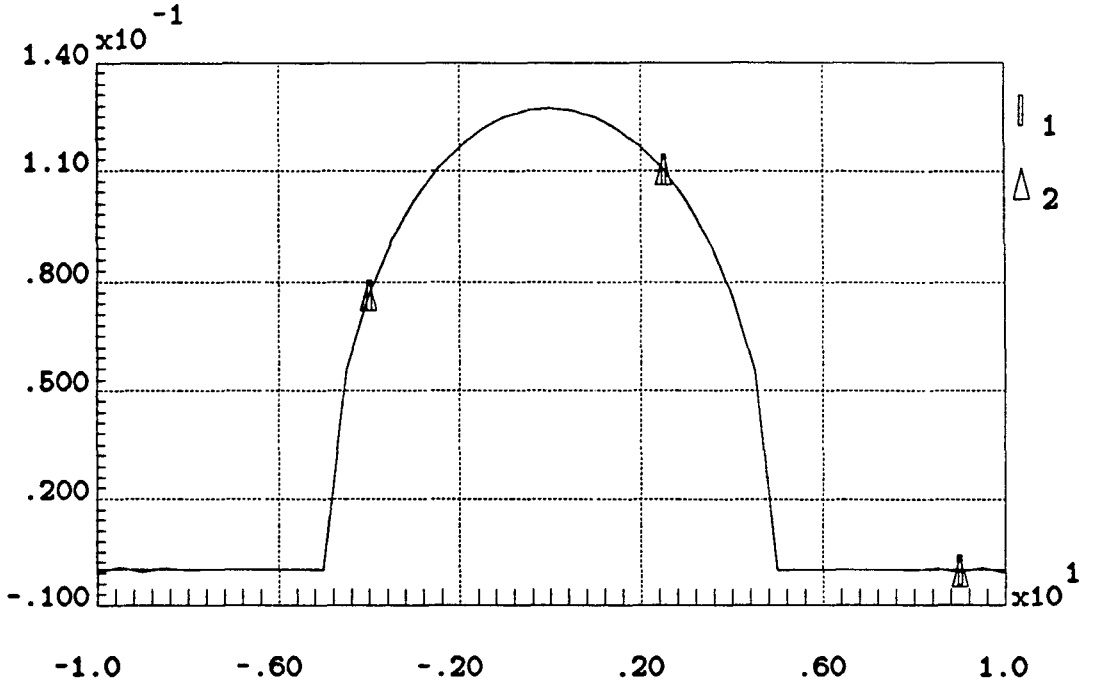

Fig.3.8a the surface stress reconstructed from the distribution of stress at $x = 1.5$

many sources that cause these errors. One of them is that the observation has been truncated. We have known that the further the point is from the area of surface load, the less is the effect of surface force on strain or stress beneath the surface is. Comparing the distributions of stress and strain for the same load, e.g. Fig.3.6a and Fig.3.6c, we find that the effect on the strain is spatially broader than the stress. Thus, more information will be lost when we truncate the observation which is expressed as strain instead of stress. Above argument can be illustrated by Fig.3.8a and Fig.3.8b, in which the number of element of sensors is only 41.

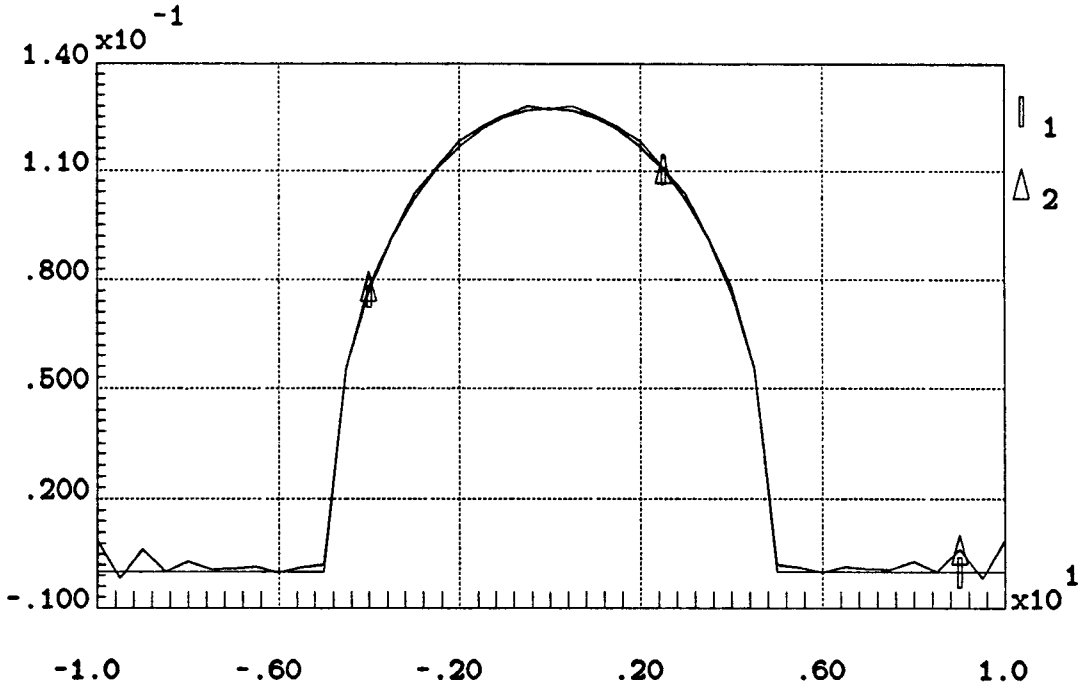

Fig.3.8b the surface stress reconstructed from the distribution of strain at $x = 1.5$

CHAPTER

FOUR

THE REGULARIZATION APPROACH FOR THE INVERSE PROBLEM

The inverse problem arising from chapter 2 can be considered in a general setting – the problem of solving an integral equation of the first kind. Many works have been devoted to it (see the references in Hilgers 1973). In view of application, some of them are to aimed at finding algorithms for constructing an approximate solution. In this chapter, our goal is also to derive an algorithm for our inverse problem by using the regularization approach.

In section 4.1 and section 4.2, the concepts of ill-posed problem and regularization theory will be cited. In section 4.3, we shall derive the algorithm for Eq.(2.12) in which f_t is omitted. In section 4.4, under some conditions, we shall extend the algorithm from section 4.3 for Eq.(2.11), in which two unknown functions exist. In section 4.5, some examples will be given.

4.1 The Concept of Ill-posed Problem

In general, the integral equation of the first kind has the form

$$\int_{a_1}^{a_2} K(y,z)f(z)dz = g(y) \qquad a_3 \leq y \leq a_4 \tag{4.1}$$

where $f(y)$ is the unknown function in a space F, $g(y)$ is a known function in a space G, $K(y,z)$ is continuous with respect to y and has a continuous partial

derivative $\partial K/\partial y$, $a_i, i = 1,2,3,4$ are finite constant real numbers. Without loss of generality, we let $a_1 = a_3 = 0$ and $a_2 = a_4 = 1$.

Moreover, Eq.(4.1) can be considered as an operator equation:

$$Kf = g \tag{4.2}$$

where $K : F \rightarrow G$ is defined as a bounded and linear operator. In this chapter, we shall take F as the space of continuous, piece-wise differentiable functions on [0,1] with sup norm:

$$\|f\| = \sup_{y \in [0,1]} |f(y)| \qquad f \in F$$

and G as $L_2[0,1]$ with norm:

$$\|g\| = [\int_0^1 g^2(y)dx]^{1/2}$$

To solve Eq(4.2) is to find an operator, K^{-1}, such that

$$f = K^{-1}g$$

Hadamard (1923) introduced the concept of well-posed problem for Eq.(4.2). The problem of determining the solution f in the space F from the initial data g in the space G is said to be well-posed on the pair of metric spaces (F, G) if the following three conditions are satisfied:

(i) for every element $g \in G$, there exists a solution f in the space F;

(ii) the solution is unique;

(iii) the solution depends on continuously on the initial data.

The problems that do not satisfy these conditions are said to be ill-posed.

The equivalent statement of condition (iii) can be that the problem is stable on the space (F, G). It means that, for any $\epsilon > 0$, there exists $\delta(\epsilon) > 0$ such that $\|g_1 - g_2\|_G \leq \delta$ implies $\|f_1 - f_2\|_F \leq \epsilon$, where f_1 and f_2 are solutions for initial data g_1 and g_2, respectively, with g_1 and g_2 in G and f_1 and f_2 in F.

The integral equation of first kind given in Eq.(4.1) is ill-posed because the condition (iii) of well-posed problem cannot be satisfied if the norm of F and G are defined as above. The typical example is given as follows.

Consider Eq.(4.1) and suppose $f(y)$ is the solution to Eq.(4.1) with $g(y)$. Then, the function

$$\bar{f}(y) = f(y) + N sin(\omega y)$$

is a solution of Eq.(4.1) with

$$\bar{g}(y) = g(y) + N \int_0^1 K(y, z) sin(\omega z) dz$$

It is clear that for any N, if the value of ω is sufficiently great, $\|g - \bar{g}\|_G$ can be arbitrary small without affecting the change in the corresponding solutions, i.e. $\|f - \bar{f}\|_F = N$.

Physically, we may only know the observation with an accuracy δg and it may not be really necessary for us to find an exact solution. This implies that conditions (i) and (ii) can be replaced by some weaker requirements. Suppose that g is the observation of the true value g^* such that $\|g - g^*\|_G \leq \delta$. Naturally, we may hope to find an approximate solution of Eq.(4.2) in some subspace $F_0 \subseteq F$ such that $\|Kf - g\|_G \leq \delta$, for $f \in F_0$. However, not every element in F_0 can be taken as an approximate solution of Eq.(4.2) since condition (iii) may

not be satisfied in F_0. To solve this problem, the supplementary information about possible solution is required.

4.2 The Regularization Approach

V. K. Ivano (1962) defined the quasi-solution for Eq.(4.2) on a compact subset $F_c \subseteq F$ and, for $g \in G$, to be a point $f \in F_c$ for which $\|Kf - g\|$ attains a minimum on F_c. Another method is regularization method given by Tikhonov, in which the supplementary information is of qualitative nature, e.g. smoothness of the solution. In this chapter, we shall use this latter approach to solve our inverse problem numerically.

The basic concept of the regularization theory is *the regularizing operator*, which is defined as follows.

Definition 1. Suppose that the element $f_T \in F$ and $g_T \in G$ are related by $Kf_T = g_T$. An operator $R(g, \alpha)$ depending on a parameter α is called a regularizing operator for the equation $Kf = g$ in a neighborhood of $g = g_T$ if

(i) there exists a positive number δ_1 such that the operator $R(g, \alpha)$ is defined for every $\alpha > 0$ and every g in G for which

$$\|g - g_T\| \leq \delta_1$$

and

(ii) there exists a function $\alpha = \alpha(\delta)$ of δ such that, for every $\epsilon > 0$, there exists a number $\delta(\epsilon) \leq \delta_1$ such that the inclusion $g_\delta \in G$ and the inequality

$$\|g_T - g_\delta\| \leq \delta(\epsilon)$$

imply

$$\|f_T - f_\alpha\| \leq \epsilon$$

where $f_\alpha = R(g_\delta, \alpha(\delta))$.

Obviously, every regularizing operator defines a stable method of approximate construction of the solution of Eq.(4.2) if the choice for α is consistent with the accuracy of g. f_α is called as *regularized solution.* α is called as *regularization parameter.* So the problem of finding a solution of Eq.(4.2) is shifted to that of finding a regularizing operator.

To construct a regularizing operator, a functional called *stabilizer* is defined.

Definition 2. A continuous nonnegative functional, $\Omega[f]$ over a subset F_1 of F and everywhere dense in F is called stabilizer, or stabilizing functional, if

a) the exact solution, f, of initial data, g, belongs to the domain of definition of $\Omega[f]$.

b) for every positive number c, the set of elements f of F_1 for which $\Omega[f] \leq c$ is a compact subset of F_1.

The main idea of regularization is to find f in F_1 which insures $\|Kf-g\|_G = \delta$ and minimizes the functional $\Omega[f]$. This is a conditional extremum problem. A common way to solve this problem is to find f to minimize functional

$$M^\alpha[f] = \|Kf - g\|^2 + \alpha\Omega[f] \tag{4.3}$$

Tikhonov (1977) proved the existence and uniqueness of such a solution.

Theorem 1. Let K denote a continuous operator from F into G. For every element g of G and every positive parameter α, there exists an element $f_\alpha \in F_1$ for which the functional

$$M^\alpha[f] = \|Kf - g\|^2 + \alpha\Omega[f]$$

attains its lower bound:

$$\inf_{f \in F_1} M^\alpha[f] = M^\alpha[f_\alpha]$$

If K is linear and $\Omega[f]$ is quadratic, the solution f_α is unique.

Thus we can define an operator $R_1(g,\alpha)$ from G into F_1 for $\alpha > 0$, so that $f_\alpha = R_1(g,\alpha)$ minimizes the functional $M^\alpha[f]$. The following theorem from Tikhonov (1977) shows that $R_1(g,\alpha)$ is a regularization operator for Eq.(4.2).

Theorem 2. For any positive number ϵ and any function $\beta_1(\delta)$ and $\beta_2(\delta)$ in the class of functions that are nonnegative, nondecreasing and continuous on an interval $[0,\delta_1]$ such that $\beta_2(0) = 0$ and $\delta^2/\beta_1(\delta) \leq \beta_2(\delta)$, there exists a number $\delta_0 = \delta_0(\epsilon,\beta_1,\beta_2) \leq \delta_1$ such that for $g \in G$ and $\delta \leq \delta_0$ the inequality $\|g - g^T\| \leq \delta$ implies the inequality $\|f_\alpha - f_T\| \leq \epsilon$, where $f_\alpha = R_1(g,\alpha)$ for all α satisfying the inequalities

$$\frac{\delta^2}{\beta_1(\delta)} \leq \alpha \leq \beta_2(\delta).$$

This theorem implies that whereas the problem described in Eq.(4.2) does not have the property of stability, the problem of minimizing the functional $M^\alpha[f]$ is stable under small changes of members of G. The choice of stabilizing functional, $\Omega[f]$, is often determined by the physical problem. This choice may not be unique. In this chapter, we shall apply the stabilizing functional of second order which has the form

$$\Omega[f] = \int_0^1 q_0(y)f^2(y) + q_1(y)(\frac{df}{dy})^2 dy$$

The choice of this functional is to seek an approximate solution which minimize $\|Kf - g\|_G$ with the aid of the smoothest functions up to order two.

It should be noted that the value of the regularization parameter α plays important role in regularization method. The admissible value of this parameter depends essentially on the information available regarding the approximate

initial data. In regularization theory, Tikhonov provided several methods to obtain α. In this chapter, we shall not discuss how to get α, but focus on the algorithm to find f which minimizes $M^{\alpha}[f]$ with given α.

4.3 An Algorithm to Solve the Equation of First Kind

By means of variational principle, one can easily prove that the unique minimizer of Eq.(4.2) must satisfy

$$K^*Kf + \alpha q_0 f - \alpha(q_1 f')' = K^*g \tag{4.4}$$

$$f'(0) = f'(1) = 0$$

where K^* is the adjoint operator of K.

Hilgers (1973) gave an algorithm to find closed form of f from Eq.(4.4) by choosing $q_0 \equiv 0$ and $q_1 \equiv 1$. To solve Eq.(4.1), this choice require that $K(x,y) \geq K_0 > 0$, where K_0 is a constant. However, our kernel given in chapter 2 does not satisfy this condition. Here, we present an algorithm to obtain f in closed form with $q_0 \equiv 1$ and $q_1 \equiv 1$. Under above conditions, Eq.(4.4) becomes

$$K^*Kf + \alpha f - \alpha f'' = K^*g \tag{4.5}$$

$$f'(0) = f'(1) = 0$$

Defining

$$h = f'$$

and

$$G(x,y) = \begin{cases} 0, & \text{if } x \leq y; \\ 1, & \text{if } x > y, \end{cases} \tag{4.6}$$

we have

$$f(y) - f(0) = \int_0^y h(x)dx = \int_0^1 G(y,x)h(x)dx.$$

or

$$f(y) = (\mathcal{G}h)(y) + c$$

where $\mathcal{G}$ is integral operator defined by Eq.(4.6), $c = f(0)$. (Note that we will use G to express a function in the rest of this chapter.) Then Eq.(4.5) becomes:

$$(K^*K + \alpha I)(\mathcal{G}h + c) - \alpha h' = K^*g$$

or

$$\alpha h' = (K^*K + \alpha I)\mathcal{G}h + cK^*b + \alpha c - K^*g \tag{4.7}$$

where I is the identity operator and

$$b(y) = \int_0^1 K(y,x)dx. \tag{4.8}$$

Integrating Eq.(4.7) from y to 1 , denoting the adjoint operator of $\mathcal{G}$ by $\mathcal{G}^*$ and applying the condition of $f'(y)$ at the boundary, we have

$$-\alpha h(y) = \mathcal{G}^*[(K^*K + \alpha I)\mathcal{G}h + c(K\mathcal{G})^*b + \alpha cd - (K\mathcal{G})^*g$$

or

$$[\mathcal{G}^*(K^*K + \alpha I)\mathcal{G} + \alpha I]h = (K\mathcal{G})^*g - c(K\mathcal{G})^*b - \alpha cd$$

where

$$d(y) = \int_0^1 G(x,y)dx \tag{4.9}$$

It then follows

$$h = [(K\mathcal{G})^*(K\mathcal{G}) + \alpha\mathcal{G}^*\mathcal{G} + \alpha I]^{-1}[(K\mathcal{G})^*(g - cb) - \alpha cd] \tag{4.10}$$

and

$$f = \mathcal{G}[(K\mathcal{G})^*(K\mathcal{G}) + \alpha\mathcal{G}^*\mathcal{G} + \alpha I]^{-1}[(K\mathcal{G})^*(g - cb) - \alpha cd] + c \qquad (4.11)$$

In order to find the constant c, define

$$h(y) = u(y) - cv(y)$$

where

$$u(y) = [(K\mathcal{G})^*(K\mathcal{G}) + \alpha\mathcal{G}^*\mathcal{G} + \alpha I]^{-1}(K\mathcal{G})^*g(y)$$

and

$$v(y) = [(K\mathcal{G})^*(K\mathcal{G}) + \alpha\mathcal{G}^*\mathcal{G} + \alpha I]^{-1}[(K\mathcal{G})^*b + \alpha d](y)$$

Since $h(0) = h(1) = 0$ from (4.4) , we have

$$u(0) - cv(0) = 0$$

and

$$u(1) - cv(1) = 0$$

Next, we shall apply the simple lemma, which has been proved by Hilgers (1973).

Lemma: For every a $\in L_2[0,1]$, we have

(i) $[(K\mathcal{G})^*a](0) = (a,b) = \int_0^1 a(x)b(x)dx$

(ii)$[(K\mathcal{G})^*a](1) = 0.$

From the definition of $u(y)$ and $v(y)$, we have

$$\alpha u(y) = (\mathcal{G}^*\mathcal{G} + I)^{-1}[(K\mathcal{G})^*(g - (K\mathcal{G})u)](y)$$

and

$$\alpha v(y) = (\mathcal{G}^*\mathcal{G} + I)^{-1}[((K\mathcal{G})^*b + \alpha d) - (K\mathcal{G})^*(K\mathcal{G})v](y)$$

Applying above lemma and noting that $d(1) = 0$ and $d(0) = 1$, we have

$$\alpha u(0) = (\mathcal{G}^*\mathcal{G} + I)^{-1}[(g,b) - ((K\mathcal{G})u, b)], \qquad u(1) = 0$$

and

$$\alpha v(0) = (\mathcal{G}^*\mathcal{G} + I)^{-1}[(b,b) - ((K\mathcal{G})u, b) + \alpha], \qquad v(1) = 0$$

It follows

$$c = \frac{(g,b) - ((K\mathcal{G})u, b)}{(b,b) - ((K\mathcal{G})v, b) + \alpha} \tag{4.12}$$

In (Hilgers 1973), it has been proved that $(b,b) - ((K\mathcal{G})v, b)$ cannot be zero. Since $\alpha > 0$, the denominator of c cannot be zero, either.

To obtain the numerical solution of Eq.(4.1), we need to discretize Eq.(4.11) and (4.12). By using the mid-point rule of integration method, the discretized version of Eq.(4.1) is

$$g(y_j) = \sum_{i=1}^{N} K(y_j, x_i) f(x_i) \delta x$$

where δx is the integral step-size. or, briefly,

$$g_j = \sum_{i=1}^{N} K_{ji} f_i \qquad j = 1, 2, ..., N \tag{4.13}$$

where $g_j = g(y_j)$, $f_i = f(x_i)$ and $K_{ji} = K(y_j, x_i)\delta x$. The matrix version of (4.13) is

$$\mathbf{g} = \mathbf{K}\mathbf{f}$$

where $\mathbf{g}$ and $\mathbf{f}$ in R^N and $\mathbf{K} \in R^{N\times N}$. Using above notation, the discretized expression of (4.11) and (4.12) are

$$\mathbf{f} = \mathbf{G}[(\mathbf{KG})^T(\mathbf{KG}) + \alpha\mathbf{G}^T\mathbf{G} + \alpha I]^{-1}[(\mathbf{KG})^T(\mathbf{g} - c\mathbf{b}) - \alpha c\mathbf{d}] + c \qquad (4.14)$$

and

$$c = \frac{\mathbf{g}^T\mathbf{b} - (\mathbf{KGu})^T\mathbf{b}}{\mathbf{b}^T\mathbf{b} - (\mathbf{KGv})^T\mathbf{b} + \alpha} \qquad (4.15)$$

where

$$\mathbf{G} = \begin{pmatrix} \delta x & 0 & \dots & 0 \\ \delta x & \delta x & \dots & 0 \\ \vdots & \vdots & \ddots & \vdots \\ \delta x & \delta x & \dots & \delta x \end{pmatrix}$$

the elements of $\mathbf{b} \in R^N$ is

$$\mathbf{b}_i = \sum_{j=1}^{N} \mathbf{K}_{ij}$$

the elements of $\mathbf{d} \in R^N$ is

$$\mathbf{d}_i = \sum_{j=1}^{N} \mathbf{G}_{ji}$$

and the vectors $\mathbf{u}$ and $\mathbf{v}$ are

$$\mathbf{u} = [(\mathbf{KG})^T(\mathbf{KG}) + \alpha\mathbf{G}^T\mathbf{G} + \alpha I]^{-1}(\mathbf{KG})^T\mathbf{g}$$

and

$$\mathbf{v} = [(\mathbf{KG})^T(\mathbf{KG}) + \alpha\mathbf{G}^T\mathbf{G} + \alpha I]^{-1}[(\mathbf{KG})^T\mathbf{b} + \alpha\mathbf{d}]$$

In the last section of this chapter, a numerical example will be given using Eq.(4.14) and (4.15).

4.4 An Algorithm for the Inverse Problem with Two Unknown Functions

In the previous section, we applied the regularization method to solve Eq.(2.12), in which only one unknown function exists. In this section, we will extend it to solve the problem with two unknown functions . This problem is of interest to us because in the process of lifting an object by a multifingered robot hand, there must exist vertical and tangential force simultaneously. It is obvious that it is not sufficient to determine two unknown functions by one observation. Extra information related to these functions is needed. In chapter 3, we studied this problem with the knowledge of smoothness of the surface in average and the assumption of constant tangential surface force. These conditions may be too strong to be applied in practice. For example, physically, the value of the coefficient of static friction at the boundary of the friction cone depends not only on the material of finger pad, but also on the material of grasped object. Hence, we have to know what the material of the object is before grasping.

We have known that the present technology of constructing the tactile sensor provides the possibility to measure the strains within an elastic material in three independent directions[]. Therefore, in this section, it is supposed that we can observe the strain profile beneath the surface of an elastic half-space in x and y directions, respectively. Moreover, we suppose that the Poisson's ratio $\nu \neq 0.5$ because, otherwise, the strains in x and y direction will be same except for sign as we have mentioned in chapter 2. Under these assumptions, we can solve the inverse problem described by Eq.(2.9) and (2.10) by applying a regularization method.

Consider the integral equations

$$\int_0^1 [K_{11}(y,x)f_1(x) + K_{12}(y,x)f_2(x)]dx = g_1(y) \tag{4.16a}$$

$$\int_0^1 [K_{21}(y,x)f_1(x) + K_{22}(y,x)f_2(x)]dx = g_2(y) \tag{4.16b}$$

where $f_i(x), i = 1,2$, are unknown functions in $L_\infty[0,1]$ and $g_i(y), i = 1,2$, are given functions in $L_2[0,1]$. In sake of convenience, we write above equations in the form of operator equations:

$$K_{11}f_1 + K_{12}f_2 = g_1$$

$$K_{21}f_1 + K_{22}f_2 = g_2$$

where K_{ij} is the integral operator from $L_\infty[0,1]$ to $L_2[0,1]$, or, more briefly,

$$\bar{K}\bar{f} = \bar{g} \tag{4.17}$$

where

$$\bar{K} = \begin{pmatrix} K_{11} & K_{12} \\ K_{21} & K_{22} \end{pmatrix}$$

and $\bar{f} = (f_1 \;\; f_2)^T, \bar{g} = (g_1 \;\; g_2)^T$. $\bar{K}$ can be considered as the 2×2 matrix integral operator, $\bar{K} : L_\infty^2[0,1] \to L_2^2[0,1]$. The norm defined on $L_\infty^2[0,1]$ is

$$\|\bar{f}(\cdot)\| = [(\sup_{x\in[0,1]} |f_1(x)|)^2 + (\sup_{x\in[0,1]} |f_2(x)|)^2]^{1/2}.$$

The norm defined on $L_2^2[0,1]$ is

$$\|\bar{g}(\cdot)\| = [\int_0^1 g_1^2(x)dx + \int_0^1 g_2^2(x)dx]^{1/2}.$$

As Eq.(4.2), Eq.(4.17) leads to an ill-posed problem. Applying the regularization method, we hope to find a $\bar{f}$ for given $\bar{g}$ to minimize the functional

$$M^{\alpha}[\bar{f}] = \|\bar{K}\bar{f} - \bar{g}\|^2 + \alpha\Omega[\bar{f}] \tag{4.18}$$

where

$$\Omega[\bar{f}] = \int_0^1 [f_1^2(y) + f_2^2(y) + (df_1(y)/dy)^2 + (df_2(y)/dy)^2]dy \tag{4.19}$$

Rewrite Eq.(4.18) as follows:

$$M^{\alpha}[\bar{f}] = (K_{11}f_1 + K_{12}f_2 - g_1)^2 + (K_{21}f_1 + K_{22}f_2 - g_2)^2 + \alpha\Omega[\bar{f}] \tag{4.20}$$

By taking first variation, the minimizer of $M^{\alpha}[\bar{f}]$ must satisfy the following equations:

$$(\alpha - K_{11}^*K_{11} - K_{21}^*K_{21})f_1 - (K_{11}^*K_{12} + K_{21}^*K_{22})f_2 - \alpha f_1'' = K_{11}^*g_1 + K_{21}^*g_2 \tag{4.21a}$$

$$(\alpha - K_{12}^*K_{12} - K_{22}^*K_{22})f_2 - (K_{12}^*K_{11} + K_{22}^*K_{21})f_1 - \alpha f_2'' = K_{12}^*g_1 + K_{22}^*g_2 \tag{4.21b}$$

and

$$f_1'(0) = f_2'(0) = f_1'(1) = f_2'(1) = 0$$

where K_{ij}^* is the adjoint operator of K_{ij}. The matrix form of Eq.(4.21) is

$$(\bar{K}^*\bar{K} + I)\bar{f} - \alpha\bar{f}'' = \bar{K}^*\bar{g} \tag{4.22}$$

where

$$\bar{K}^* = \begin{pmatrix} K_{11}^* & K_{21}^* \\ K_{12}^* & K_{22}^* \end{pmatrix}$$

Using the same approach as in section 4.3, one can find $\bar{f}$ in the closed form:

$$\bar{f} = \bar{\mathcal{G}}[(\bar{K}\bar{\mathcal{G}})^*(\bar{K}\bar{\mathcal{G}}) + \alpha(\bar{\mathcal{G}}^*\bar{\mathcal{G}} + I)]^{-1}[(\bar{K}\bar{\mathcal{G}})^*(\bar{g} - \bar{B}\bar{c}) - \alpha\bar{D}\bar{c}] + \bar{c} \qquad (4.23)$$

where

$$\bar{\mathcal{G}} = \begin{pmatrix} \mathcal{G} & 0 \\ 0 & \mathcal{G} \end{pmatrix}$$

$\mathcal{G}$ is the integral operator with the kernel given by (4.6);

$$\bar{D} = \begin{pmatrix} d & 0 \\ 0 & d \end{pmatrix},$$

d is given by (4.9); the elements of $\bar{B} \in L_2^{2\times 2}[0,1]$ are

$$b_{ij}(y) = \int_0^1 K_{ij}(y,x)dx \qquad i,j = 1,2$$

and

$$\bar{c} = (f_1(0) \quad f_2(0))^T$$

By using the similar method as in section 4.3, we can get $\bar{c}$ as follows.

Let S and T be 2×2 matrices with the elements defined on $L_2[0,1]$. We define the inner production of S and T as

$$(S,T) = \begin{pmatrix} (s_{11},t_{11}) + (s_{21},t_{21}) & (s_{11},t_{12}) + (s_{21},t_{22}) \\ (s_{12},t_{11}) + (s_{22},t_{21}) & (s_{12},t_{12}) + (s_{22},t_{22}) \end{pmatrix}$$

where

$$(s_{ij},t_{kl}) = \int_0^1 s_{ij}(x)t_{kl}(x)dx \quad i,j,k,l = 1,2$$

Then $\bar{c}$ has the form:

$$\bar{c} = [(\bar{B}, \bar{B}) - ((\bar{\mathcal{K}}\bar{\mathcal{G}})\bar{V}, \bar{B}) + \alpha I]^{-1}[(\bar{B}, \bar{g}) - (\bar{B}, (\bar{\mathcal{K}}\bar{\mathcal{G}})\bar{u})] \qquad (4.24)$$

where

$$\bar{u}(y) = [(\bar{\mathcal{K}}\bar{\mathcal{G}})^*(\bar{\mathcal{K}}\bar{\mathcal{G}}) + \alpha(\bar{\mathcal{G}}^*\bar{\mathcal{G}} + I)]^{-1}(\bar{\mathcal{K}}\bar{\mathcal{G}})^*\bar{g}$$

and

$$\bar{V}(y) = [(\bar{\mathcal{K}}\bar{\mathcal{G}})^*(\bar{\mathcal{K}}\bar{\mathcal{G}}) + \alpha(\bar{\mathcal{G}}^*\bar{\mathcal{G}} + I)]^{-1}[(\bar{\mathcal{K}}\bar{\mathcal{G}})^*\bar{B} + \alpha\bar{D}].$$

In order to find a numerical solution of Eq.(4.16), Eq.(4.23) and (4.24) should be discretized. By using the mid-point rule of integration, the discretized version of Eq.(4.16) is

$$g_1(y_j) = \sum_{i=1}^{N}[K_{11}(y_j, x_i)f_1(x_i) + K_{12}(y_j, x_i)f_2(x_i)]\delta x \qquad (4.25a)$$

$$g_2(y_j) = \sum_{i=1}^{N}[K_{21}(y_j, x_i)f_1(x_i) + K_{22}(y_j, x_i)f_2(x_i)]\delta x \qquad (4.25b)$$

for $j = 1, 2, ..., N$. The matrix versions of above two equations are

$$\mathbf{g}_1 = \mathbf{K}_{11}\mathbf{f}_1 + \mathbf{K}_{12}\mathbf{f}_2$$

$$\mathbf{g}_2 = \mathbf{K}_{21}\mathbf{f}_1 + \mathbf{K}_{22}\mathbf{f}_2$$

where $\mathbf{g}_i$ and $\mathbf{f}_i, i = 1, 2$, are in R^N and $\mathbf{K}_{ij} \in R^{N\times N}$. For short, above equations can be

$$\bar{\mathbf{g}} = \bar{\mathbf{K}}\bar{\mathbf{f}}$$

where $\bar{\mathbf{g}} = (\mathbf{g}_1^T \quad \mathbf{g}_2^T)^T, \bar{\mathbf{f}} = (\mathbf{f}_1^T \quad \mathbf{f}_2^T)^T$ and

$$\bar{\mathbf{K}} = \begin{pmatrix} \mathbf{K}_{11} & \mathbf{K}_{12} \\ \mathbf{K}_{21} & \mathbf{K}_{22} \end{pmatrix}$$

By using above notation, the discretized expression of Eq.(4.23) and (4.24) are

$$\bar{\mathbf{f}} = \bar{\mathbf{G}}[(\bar{\mathbf{K}}\bar{\mathbf{G}})^T(\bar{\mathbf{K}}\bar{\mathbf{G}}) + \alpha(\bar{\mathbf{G}}^T\bar{\mathbf{G}} + \mathbf{I})]^{-1}[(\bar{\mathbf{K}}\bar{\mathbf{G}})^T(\bar{\mathbf{g}} - \bar{\mathbf{B}}\bar{\mathbf{c}}) - \alpha\bar{\mathbf{D}}\bar{\mathbf{c}}] + \bar{\mathbf{c}} \qquad (4.26)$$

and

$$\bar{\mathbf{c}} = [\bar{\mathbf{B}}^T\bar{\mathbf{B}} - (\bar{\mathbf{K}}\bar{\mathbf{G}}\bar{\mathbf{V}})^T\bar{\mathbf{B}}) + \alpha\mathbf{I}]^{-1}[\bar{\mathbf{B}}^T\bar{\mathbf{g}} - \bar{\mathbf{B}}^T(\bar{\mathbf{K}}\bar{\mathbf{G}}\bar{\mathbf{u}})] \qquad (4.27)$$

where

$$\bar{\mathbf{G}} = \begin{pmatrix} \mathbf{G} & 0 \\ 0 & \mathbf{G} \end{pmatrix}$$

$\mathbf{G}$ is same as one expressed in (4.15);

$$\bar{\mathbf{D}} = \begin{pmatrix} \mathbf{d} & 0 \\ 0 & \mathbf{d} \end{pmatrix}$$

$\mathbf{d} \in R^N$ is the same as one expressed in (4.16);

$$\bar{\mathbf{B}} = \begin{pmatrix} \mathbf{B}_{11} & \mathbf{B}_{12} \\ \mathbf{B}_{21} & \mathbf{B}_{22} \end{pmatrix}$$

in which $\mathbf{B}_{ij} \in R^N$ is the summation of columns of matrix $\mathbf{K}_{ij}$;

$$\bar{\mathbf{u}} = [(\bar{\mathbf{K}}\bar{\mathbf{G}})^T(\bar{\mathbf{K}}\bar{\mathbf{G}}) + \alpha(\bar{\mathbf{G}}^T\bar{\mathbf{G}} + \mathbf{I})]^{-1}(\bar{\mathbf{K}}\bar{\mathbf{G}})^T\bar{\mathbf{g}}$$

and

$$\bar{\mathbf{V}} = [(\bar{\mathbf{K}}\bar{\mathbf{G}})^T(\bar{\mathbf{K}}\bar{\mathbf{G}}) + \alpha(\bar{\mathbf{G}}^T\bar{\mathbf{G}} + \mathbf{I})]^{-1}[(\bar{\mathbf{K}}\bar{\mathbf{G}})^T\bar{\mathbf{B}} + \alpha\bar{\mathbf{D}}]$$

4.5 Numerical Examples

In this section, we will use the algorithms given by above two sections to our inverse problem arising from chapter 2. For the sake of convenience, we rewrite Eq.(2.9) and Eq.(2.10) in following forms

$$\int_{-\infty}^{\infty}[K_{x1}(y-y_0)f_v(y_0)+K_{x2}(y-y_0)f_t(y_0)]dy_0=\epsilon_x(y) \tag{4.28a}$$

$$\int_{-\infty}^{\infty}[K_{y1}(y-y_0)f_v(y_0)+K_{y2}(y-y_0)f_t(y_0)]dy_0=\epsilon_y(y) \tag{4.28b}$$

$y \in R$. Here, the superscript 'strain' and variable x are omitted. In the following examples, we choose $x = 1.5$ and the Poisson's ratio $\nu = 0.45$. The kernels $K_{x1}(y), K_{x2}(y), K_{y1}(y)$ and $K_{y2}(y)$ are given in Eq.(2.9) and (2.10).

Applying the assumptions of $g(y)$ and $f(y)$ given in chapter 2, Eq.(4.28) can be approximately expressed as

$$\int_{-A}^{A}[K_{x1}(y-y_0)f_v(y_0)+K_{x2}(y-y_0)f_t(y_0)]dy_0=\epsilon_x(y) \tag{4.29a}$$

$$\int_{-A}^{A}[K_{y1}(y-y_0)f_v(y_0)+K_{y2}(y-y_0)f_t(y_0)]dy_0=\epsilon_y(y) \tag{4.29b}$$

for $y \in [-A, A]$, where A is the half width of surface of the finger. Now Eq.(4.14) and Eq.(4.15) or Eq.(4.26) and Eq.(4.27) can be applied immediately to solve above integral equations. In following examples, $E = 1$ and the number of elements of sensors $N = 81$. We suppose the rigid load is cylinder. The designed surface stress for this load is

$$f_v(y)=\begin{cases}\frac{2P}{\pi a^2}\sqrt{a^2-y^2} & \text{for } y \in [-a,a];\\ 0, & \text{otherwise,}\end{cases}$$

where a is the half-width of the contact region and P is the force per length.

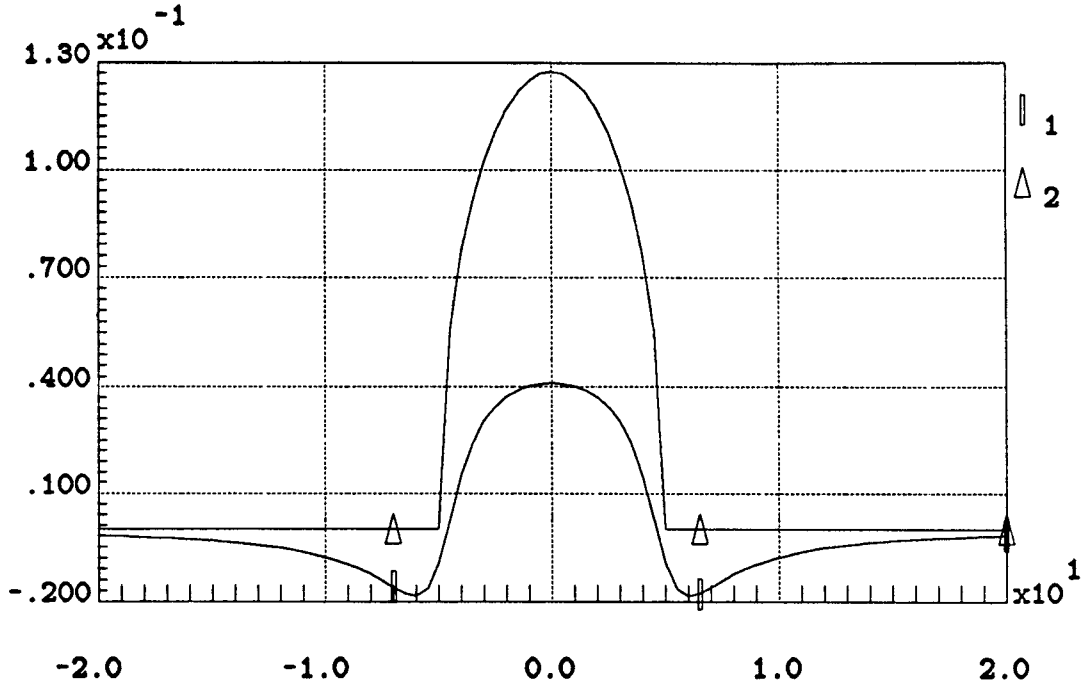

Fig.4.1a 1. the strain at $x = 1.5$; 2. the designed surface stress

Example 4.1 Cylinder indenting without friction.

Fig.4.1a shows the designed surface stress profile and the strain profile, $\epsilon_x(y)$, beneath the surface at $x = 1.5$. By choosing the regularization parameter $\alpha = 10^{-3}$ and 10^{-4} and applying Eq.(4.14) and Eq.(4.15), we get Fig.4.1b and Fig.4.1c, in which the designed and reconstructed surface stress profiles for two different α are shown.

Example 4.2 Cylinder indenting with friction.

In this example, let $f_t(y)$ satisfy

$$f_t(y) = 0.5 f_v(y).$$

Fig.4.2a shows the designed surface stress profiles, $f_v(y), f_t(y)$ and the strain profiles, $\epsilon_x(y), \epsilon_y(y)$, beneath the surface at $x = 1.5$. By choosing the regularization parameter $\alpha = 10^{-3}$ and 10^{-4} and applying Eq.(4.26) and Eq.(4.27), we get Fig.4.2b and Fig.4.2c, in which the designed and reconstructed surface stress profiles for two different α are shown.

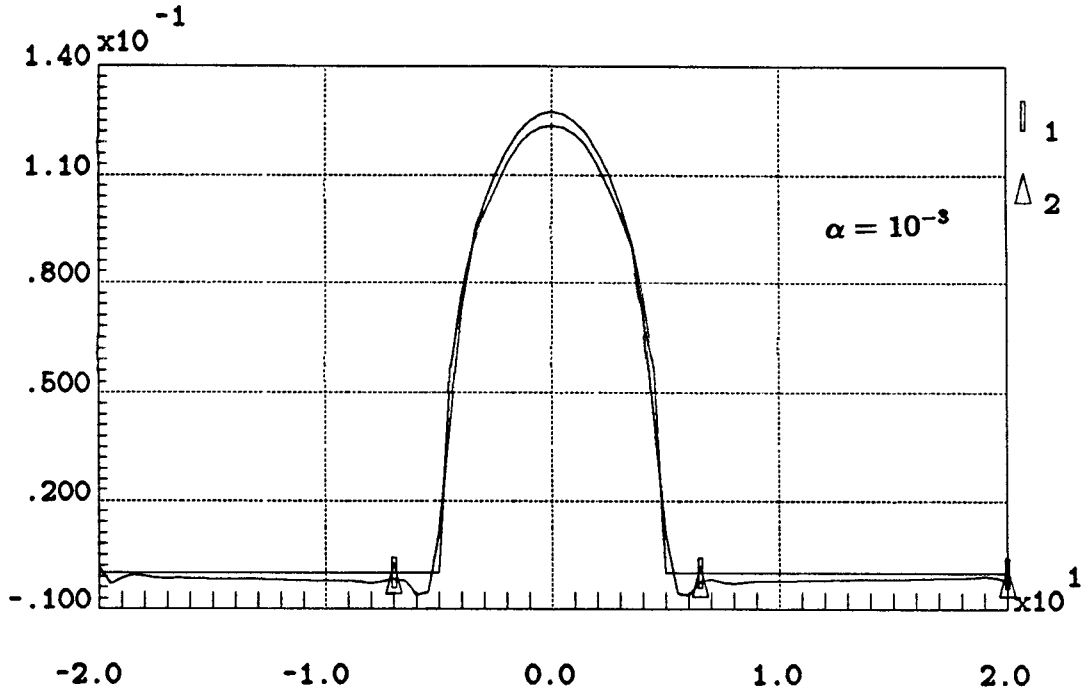

fig.4.1b 1. the designed surface stress; 2. the reconstructed surface stress.

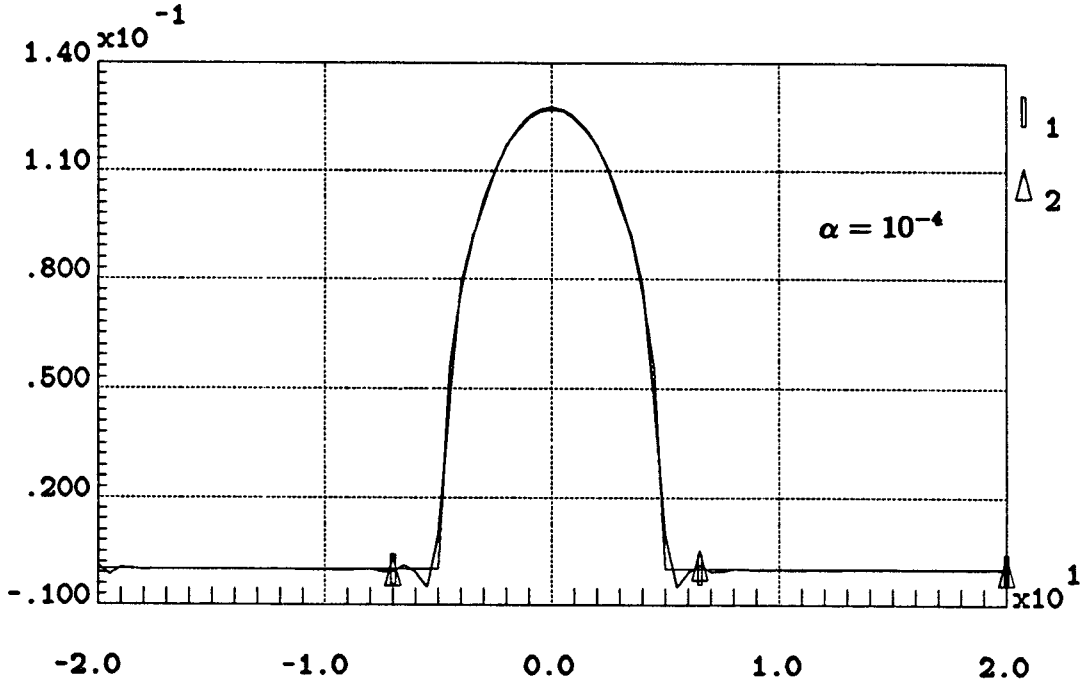

fig.4.1c 1. the designed surface stress; 2. the reconstructed surface stress.

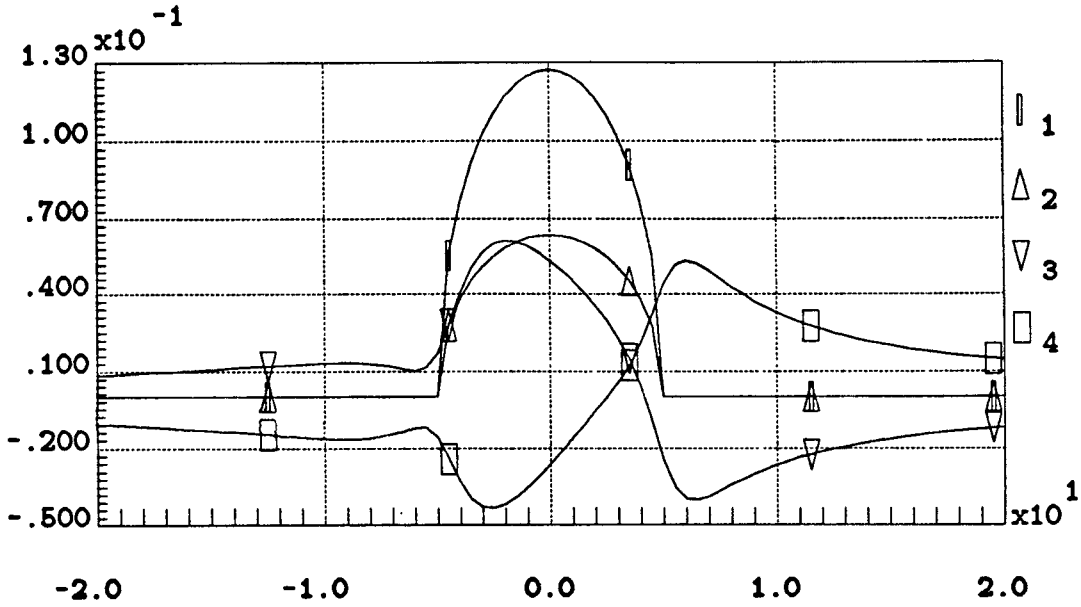

Fig.4.2a 1. the designed vertical surface stress;
2. the designed tangential surface stress;
3. the strain ϵ_x at $x = 1.5$;
4. the strain ϵ_y at $x = 1.5$.

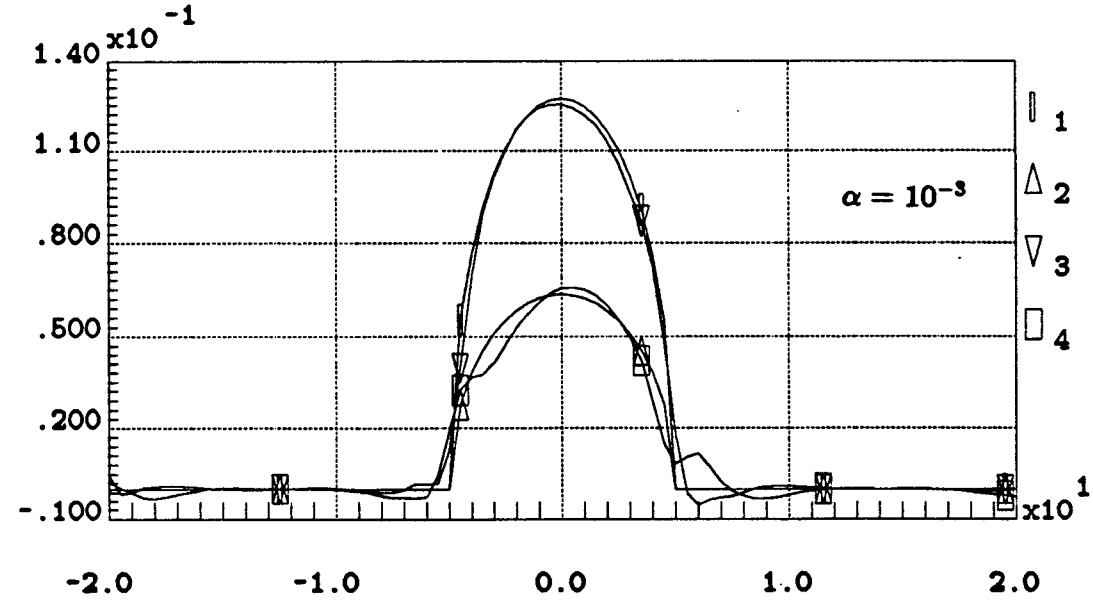

Fig.4.2b 1. the designed vertical surface stress;
2. the designed tangential surface stress;
3. the reconstructed vertical surface stress;
4. the reconstructed tangential surface stress.

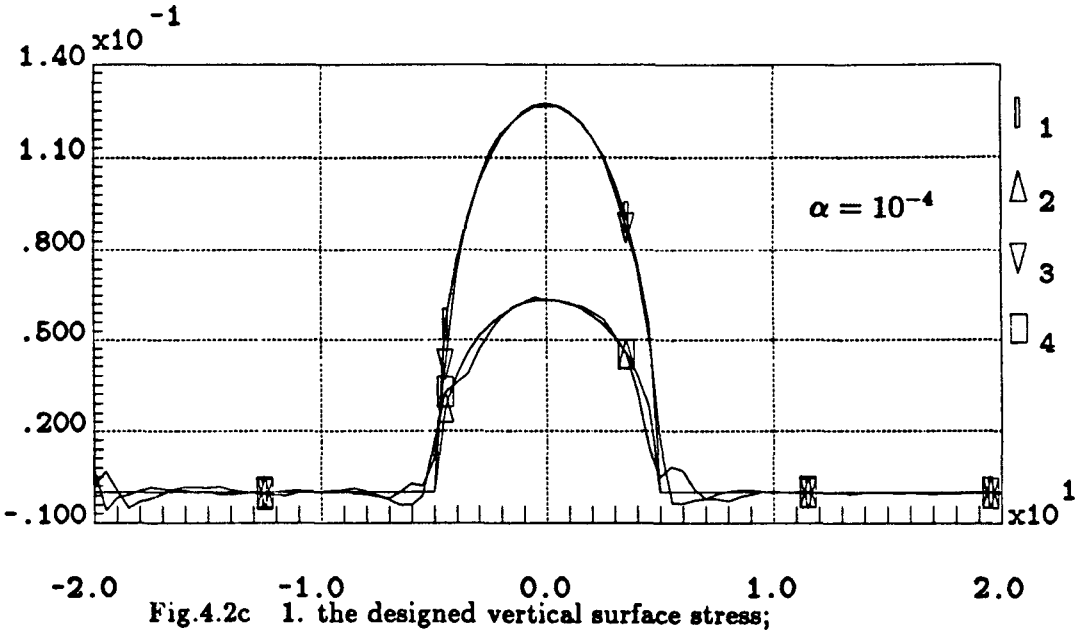

Fig.4.2c 1. the designed vertical surface stress;
2. the designed tangential surface stress;
3. the reconstructed vertical surface stress;
4. the reconstructed tangential surface stress.

Remark: Suppose $\nu = 0.5$ and suppose that arrays of sensors which can be mounted on two horizontal layers in two different depths beneath the surface can be constructed. That means we can observe strain profiles at two depths beneath the surface. In this case, we also get two independent integral equations. By using the same method as example 4.2, one can find the satisfied solution.

CHAPTER
FIVE

ANALOG NETWORKS FOR THE INVERSE PROBLEM

In the previous chapters, we derived numerical methods to solve the inverse problem. Some examples were displayed. Although these methods are noniterative, they are in their original form unsuitable for real time calculation. For this reason, analog networks are developed for both Fourier inversion and regularization based methods. As computed by these networks, the results are spatially discrete, but they can be obtained immediately after the observations are input to the network. In this chapter, we shall study the application of analog network realization to regularization based methods for the inverse problem described in chapter 2.

5.1 Equivalence of Analog Networks and Regularization

From Hamilton's principle of least action, we know that the behaviors of many physical systems are equivalent in the sense of minimizing an associated action functional. Electrical networks can be considered as natural computational models for solving these minimizing processes. In this section we will demonstrate that both the regularization principle and the minimum power principle for an electrical network consisting of resistances and sources are equivalent to a quadratic minimization problem in Hilbert space. It should be mentioned that Poggio and Koch (1985) gave a proof of this idea, but their argument for the

above equivalence appears to be incomplete. We give a complete proof below.

Consider the integral equation

$$\int_0^1 K(x,y)f(y)dy = g(x), \qquad 0 \leq x \leq 1 \tag{5.1}$$

where K is an L_2-kernel, f and g are in $L_2[0,1]$ and f is piece-wise differentiable on $[0,1]$. As usual, the norm of any element in $L_2[0,1]$ is defined as

$$\|f\| = < f, f >^{1/2} = (\int_0^1 f^2(x)dx)^{1/2}$$

It can be shown that, for the space considered here, Eq.(5.1) is still ill-posed in the sense of Hadamard.

From chapter 4, we know that the basic idea of regularization methods for solving Eq.(5.1) is to restrict the space of possible solutions by choosing the function f that minimizes the functional

$$M^\alpha[f] = \| \int_0^1 K(x,y)f(y)dy - g(x)\|^2 + \alpha\Omega[f] \tag{5.2}$$

where α is called the regularization parameter, $\Omega[f]$ is the stabilizing functional defined in chapter 4, which we chose as the functional of second order

$$\Omega[f] = \int_0^1 f^2(y) + (df(y)/dy)^2 dy \tag{5.3}$$

In a more general sense, we write (5.2) with (5.3) in the form

$$M^\alpha[f] = \|Kf - g\|^2 + \alpha\|Pf\|^2 \tag{5.4}$$

where K and P are linear operators, P may be densely defined.

As denoted by Poggio and Koch (1985) , regularization principles of the form (5.4) are equivalent to quadratic minimization problem in a Hilbert space.

In fact, we can rewrite (5.4) in terms of inner products

$$< Kf - g, Kf - g > + \alpha < Pf, Pf > \tag{5.5}$$

Denoting K^* and P^* as the adjoint operators K and P, respectively, (5.5) can be expressed as

$$< f, K^*Kf > - 2 < f, K^*g > + \alpha < f, P^*Pf > + < g, g > \tag{5.6}$$

Then, by disregarding the constant term, the regularization problem is equivalent to minimizing the following quadratical functional

$$< f, Qf > - 2 < f, K^*g > \tag{5.7}$$

where $Q = \alpha P^*P + K^*K$. It is clear that P may be chosen so that Q is positive definite.

We next prove that the minimum power principle for an electrical network consisting of resistances and sources is also a quadratic minimization problem. Suppose we have an electrical network consisting of resistances, r_k for $k = 1, \ldots, b$, and voltage sources e_{si}, for $i = 1, \ldots, l$, where b is the number of branches of the whole network, l is the number of independent loops. Denote the branch currents and voltages as elements in the column vectors $\vec{j} = [j_1, \ldots, j_b]^T$ and $\vec{v} = [v_1, \ldots, v_b]^T$. By Ohm's law, we have

$$A\vec{j} = \vec{v} \tag{5.8}$$

where $A = diag[r_1, \ldots, r_b]$. As is well known, the constraints among v_k are derived from Kirchhoff's voltage-law. These constraints are l in number as follows

$$\begin{pmatrix} \beta_{11} & \beta_{12} & \cdots & \beta_{1b} \\ \beta_{21} & \beta_{22} & \cdots & \beta_{2b} \\ \vdots & \vdots & \ddots & \vdots \\ \beta_{l1} & \beta_{l2} & \cdots & \beta_{lb} \end{pmatrix} \begin{pmatrix} v_1 \\ v_2 \\ \vdots \\ v_b \end{pmatrix} = \begin{pmatrix} e_{s1} \\ e_{s2} \\ \vdots \\ e_{sl} \end{pmatrix} \tag{5.9}$$

where β_{ij} is 0 or $+1$ or -1. Or briefly,

$$B\bar{v} = \bar{e}_s \tag{5.9}'$$

If we select a tree in the network graph and if the corresponding link-branches are numbered consecutively from 1 to l, then, by suitably choosing the reference directions of independent loops, B can be set in canonic form

$$B = [I_l \vdots \bar{B}]$$

where $I_l \in R^{l\times l}$, $\bar{B} \in R^{l\times n}$, $n = b - l$ and $n + 1$ is the number of the nodes of the tree of the network. If we choose the link-branch currents $j_1, \ldots, j_l$ as loop currents, $i_1, \ldots, i_l$, it is not difficult to prove (see Guillemin 1963) that the relation between loop currents and voltage sources is

$$R\bar{i} = \bar{e}_s \tag{5.10}$$

where $\bar{i} = [i_1, \ldots, i_l]^T$, and

$$R = A_l + \bar{B}A_n\bar{B}^T$$

$A_l \in R^{l\times l}$ and $A_n \in R^{n\times n}$ are submatrices of A such that $A = block\ diag[A_l, A_n]$.

Premultiplying Eq.(5.10) by transpose of $\bar{i}$, we have

$$\bar{i}^T R\bar{i} = \bar{i}^T\bar{e}_s \tag{5.11}$$

By the definition of $\bar{i}$ and $\bar{e}_s$, we know that i_k is the current delivered by e_{ks}. Hence, the right hand side of Eq.(5.11) is the total power, P, produced by sources. It is easy to see from the law of conservation of energy that the left hand side is the power dissipated by resistances. Denoting

$$2F = \bar{i}^T R \bar{i} = \sum_{s,k=1}^{l} R_{sk} i_s i_k$$

where R_{sk} are the elements of matrix the R, and

$$P_d = \sum_{k=1}^{l} i_k e_{sk}$$

we have

$$P_d = 2F \tag{5.12}$$

where F is called *energy function.*

The minimum power principle states that in a linear network containing ideal sources, the distribution of currents and voltages at every instant assumes values such that the total rate of energy dissipation becomes a minimum, subject to the constraint that energy for the whole system is conserved. In other words, the distribution of the currents should minimize F under the constraint $P_d = 2F$. This is a constrained minimization problem. In producing a Lagrange multiplier, the currents should minimize the functional

$$F + \lambda(P_d - 2F) \tag{5.13}$$

As usual, to minimize the functional (5.13), we have l equations

$$\frac{\partial}{\partial i_k}[F + \lambda(P_d - 2F)] = 0 \tag{5.14}$$

for $k = 1, \ldots, l$. By multiplying the separate equations (5.14) respectively by $i_1, \ldots, i_l$ and adding them together, we have

$$\sum_{k=1}^{l} \frac{\partial}{\partial i_k}[F + \lambda(P_d - 2F)]i_k = 0 \tag{5.15}$$

From the expression of F and P_d, we note that

$$P_d = \sum_{k=1}^{l} \frac{\partial P_d}{\partial i_k} i_k$$

and

$$F = \frac{1}{2} \sum_{k=1}^{l} \frac{\partial F}{\partial i_k} i_k$$

Then Eq.(5.15) becomes

$$2F + \lambda(P_d - 4F) = 0$$

or

$$2(1 - \lambda)F + \lambda(P_d - 2F) = 0 \tag{5.16}$$

Since $P_d = 2F$, Eq.(5.16) implies $\lambda = 1$. Therefore, the distribution of currents $i_1, \ldots, i_l$ should minimize the quadratic functional

$$P_d - F = \sum_{k=1}^{l} i_k e_{sk} + \frac{1}{2} \sum_{s,k=1}^{l} R_{sk} i_s i_k \tag{5.17}$$

It is obvious that by discretizing (5.7), it must has same form as (5.17).

If we write equation (5.15) more explicitly, we find that the distribution of the currents which minimize the dissipated power of the whole network just satisfies Kirchhoff's law. In fact, by solving

$$\frac{\partial}{\partial i_k}[P_d - F] = 0, \qquad k = 1, \ldots, l$$

we have

$$\sum_{s=1}^{l} R_{ks} i_s = e_{sk} \qquad k = 1, \ldots, l$$

It is the Kirchhoff loop equation, or the equilibrium equation on a loop basis. Therefore, we conclude that regularization problems can be mapped into a problem of relaxation of electrical networks.

5.2 Analog Network for Inverse Problem

In this section, we will investigate the method of minimizing functional (5.2) with (5.3) by relaxation of an analog network. Instead of discretizing Eq.(4.23) in chapter 4, we first of all discretize the functional (5.2) with (5.3) directly.

Using the norm we chose, the functional (5.2) with (5.3) is explicitly

$$\int_0^1 dx[\int_0^1 K(x,y)f(y)dy - g(x)]^2 + \alpha \int_0^1 [f'^2(y) + f^2(y)]dy \tag{5.18}$$

The discretized version of above functional is

$$\sum_{i=0}^{N} \sigma[\sum_{j=0}^{N} K_{ij} f_j - g_i]^2 + \alpha\sigma^{-1} \sum_{i=0}^{N-1} (f_{i+1} - f_i)^2 + \alpha\sigma \sum_{i=0}^{N} f_i^2$$

where $K_{ij} = K(x_i, y_j)\sigma$. This version can be expressed in matrix vector form as follows

$$\sigma(\bar{g} - K\bar{f})^T(\bar{g} - K\bar{f}) + \alpha\sigma^{-1}\bar{f}^T Q\bar{f} + \alpha\sigma\bar{f}^T\bar{f}$$

or

$$\bar{f}^T[\sigma K^T K + \alpha\sigma^{-1}Q + \alpha\sigma I]\bar{f} - 2\bar{f}^T K^T \bar{g} + \sigma\bar{g}^T\bar{g} \tag{5.19}$$

where K is formed by elements K_{ij}, $\bar{f} = (f_0, \ldots, f_N)^T, \bar{g} = (g_0, \ldots, g_N)^T$ and

$$Q = \begin{pmatrix} 1 & -1 & 0 & \ldots & 0 \\ -1 & 2 & -1 & \ldots & 0 \\ \vdots & \ddots & \ddots & \ddots & \vdots \\ 0 & \ldots & -1 & 2 & -1 \\ 0 & \ldots & 0 & -1 & 1 \end{pmatrix}$$

It is clear that (5.19) is a quadratical functional of vector $\bar{f}$. By minimizing (5.19) over $\bar{f}$, we have

$$P\bar{f} = \bar{b} \tag{5.20}$$

where

$$\bar{b} = K^T\bar{g}$$

$$P = K^T K + \alpha\sigma^{-2}Q + \alpha I$$

It is clear that P is a symmetric positive definite matrix.

Based on the results in section 5.1 and this section, we will determine an analog network to solve Eq.(5.20). Instead of using the equilibrium equations on a loop basis, we will use the equations from a node basis since the relationship of loop and node analysis is a dual one. From basic network analysis (Jensen, 1974), we have following result. Suppose we are given an electrical network which has $n+1$ nodes and has some current sources and conductances connecting these nodes such that the graph of this network is connected. After numbering the nodes from 1 to $n+1$, we choose $(n+1)$th node as the reference or ground, and denote the voltage of ith node with respect to the ground by V_i. Then we have the equilibrium equations,

$$\begin{pmatrix} g_{11} & g_{12} & \cdots & g_{1n} \\ g_{21} & g_{22} & \cdots & g_{2n} \\ \vdots & \vdots & \ddots & \vdots \\ g_{n1} & g_{n2} & \cdots & g_{nn} \end{pmatrix} \begin{pmatrix} V_1 \\ V_2 \\ \vdots \\ V_n \end{pmatrix} = \begin{pmatrix} J_1 \\ J_2 \\ \vdots \\ J_n \end{pmatrix}$$

where g_{ii} is *self-conductance* of ith node, which is defined as the sum of all conductance attached to the ith node, for $i = 1,\ldots,n$; $g_{ij} = g_{ji}, i \neq j$ is *mutual conductance* between ith and jth node, which is defined as the sum of all conductance from ith to jth node with a negative sign J_i are the current sources *entering* the ith node.

From above result, the electrical network for Eq.(5.20) can be designed as follows. Let $g_{ij} = p_{ij}$ be the mutual conductance connecting ith and jth nodes, $i \neq j$, and$i,j = 1,\ldots,n$, and $g_{ii} = p_{ii}$ be the self-conductance of ith node. Then the conductance between ith and $(n+1)th$ node $g_i = p_{ii} + \sum_{\substack{j=1 \\ j\neq i}}^{n} p_{ij}$. Moreover, let $J_i = b_i$ be the current sources entering from $(n+1)th$ node to others. By using this circuit, we can solve Eq.(5.9) by measuring the voltages between ith node and ground. As we have proved in section 5.1, this solution is the discrete minimizer of functional (5.18). Fig.5.1 shows a circuit designed by above approach, in which n=5.

It should be noted that, in the above circuit, the negative conductances, or resistances, may appear. As pointed out by Poggio and Koch (1985), there are at least three ways for implementing negative resistances by using basic circuit components. That is (i) replacing the positive and negative by inductances and capacitances with impedance $i\omega L$ and $-i(\omega C)^{-1}$ respectively; (ii) using operational amplifiers or other circuits; (iii) exploiting the negative impedance regions in a nonlinear system.

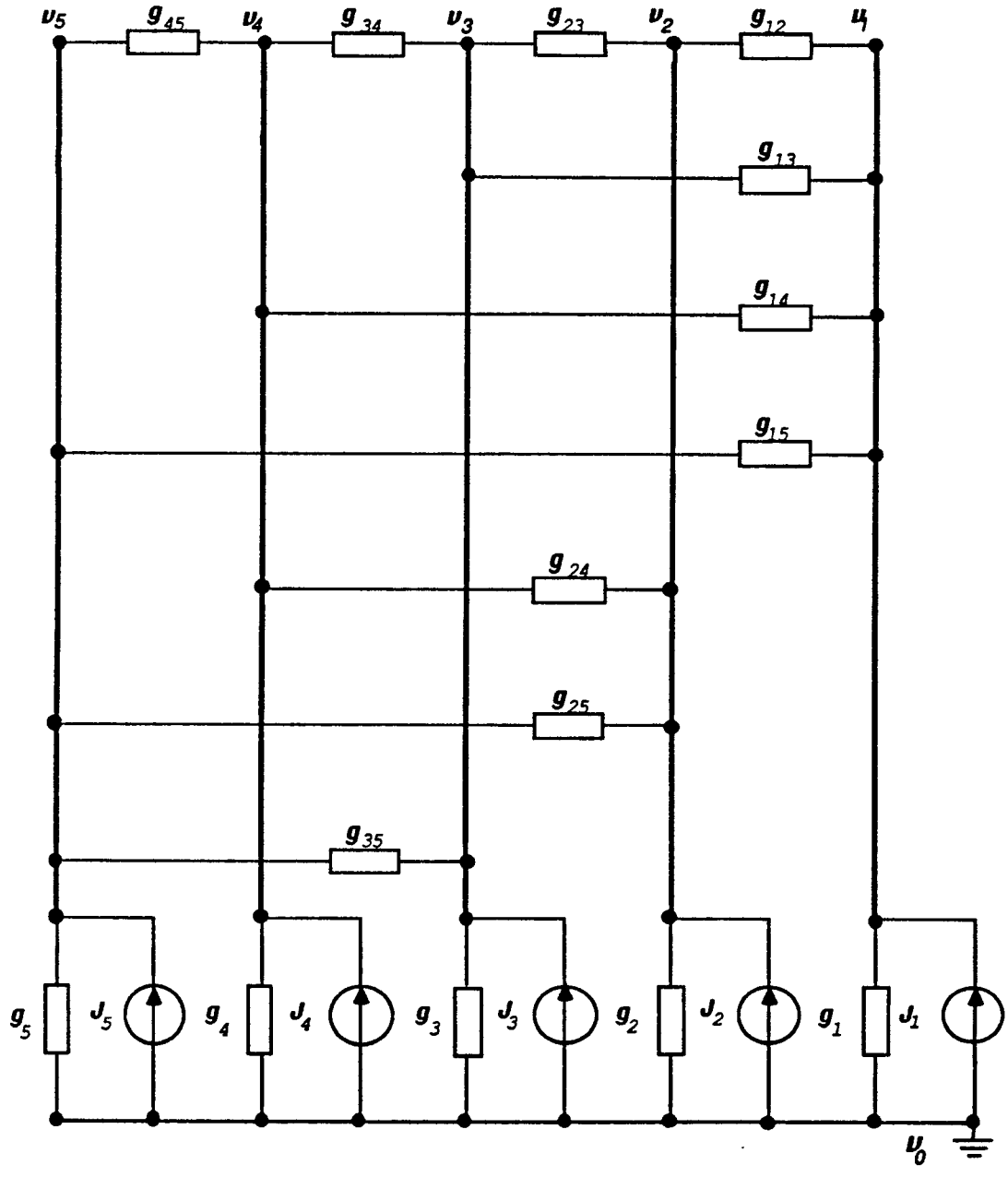

Fig.5.1 a simple network for solving the inverse problem

CHAPTER
SIX

AN APPLICATION OF TACTILE SENSORS IN STATICS OF MULTIFINGERED HAND

6.1 Definitions and Assumptions

From Salisbury(1982), a *robotic hand* is defined as an interface between the mechanical arm and the objects it interacts with, and a *multifingered hand* or *articulated hand* is defined as a device with two or more powered joints that can grip and manipulate objects. Here, we define a *multifingered hand system* as a multifingered hand together with the grasped object. For simplification, a *planar-multifingered hand system* is defined as a multifingered hand system in which the net grasping force and net external force lie in a plane defined by the contact points and center of mass of the object. In this chapter we shall study this kind of hand system. Moreover, we define the *fingertip* as the last link of every fingers, on which tactile sensors covered by some kind of elastic material are mounted.

In this chapter, we make following assumptions:

(1) the hand has two fingers and two links for every finger.

(2) the grasped object is in the *hand workspace*, which is defined as the range of possible manipulation.

(3) no sliding occurs between the fingertips and the object.

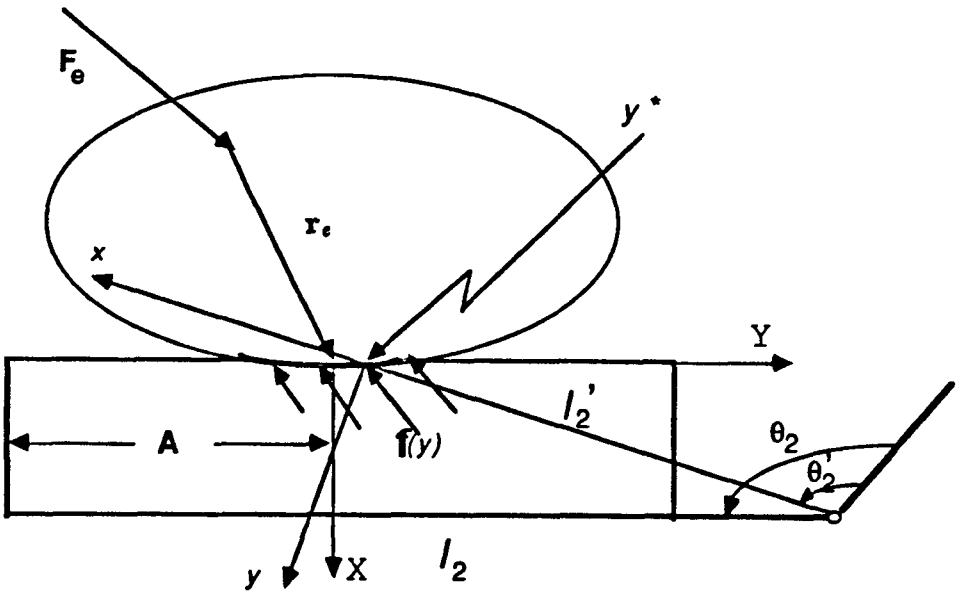

Fig.6.1 Surface contact and point contact

(4) the surface of fingertip is a plane and the surface of the object is a smooth side without vertex or wedge, and the boundary of the contact area is within the surface of fingertip.(see Fig.6.1).

(5) the tangential component of surface stress is in the same direction and is directly proportional to the magnitude of the normal surface stress.

(6) the characteristics of the elastic material satisfy the assumptions given in chapter 2 and the plane-strain assumption(see chapter 2) can be applied approximately.

(7) the stiffness of the elastic material covering the tactile sensors is large enough so that we can treat that the deformation of the fingertip is infinitesimal with respect to the dimension of the finger and the grasped object and that the fingertip is rigid when the multifingered hand system is in static state.

6.2 The Concept of Concentrated Contact Force

We have known that when a rigid object is pressed on the surface of an elastic material with a force, F, there is a distribution of stress on the surface.

By Newton's law, this stress can be expressed as the distributed force, which is defined as force per unit length, exerted on at the object over the contact area. When the object is in a stable static state, this distributed force should balance the force F. By means of the method derived from previous chapters, this distributed force can be reconstructed by tactile sensors. However, to analyze the static properties of the grasped object , it is more convenient to use concentrated forces for every contact. If the type of contact between the fingertip and the object is point contact with friction, the force at the contact is a concentrated one and the multifingered hand system becomes an articulated system with a closed loop.

In this section, we intend to transform the distributed force to equivalent concentrated force. The meaning of equivalence here is that if one substitutes the distributed force by a equivalent concentrated force, the behavior of the system is still in stable equilibrium state. The expression of this concentrated force should provide the magnitude, the direction and the location of the force with respect to the finger surface.

Suppose an external force $\mathbf{F}_e$ and a force distribution $\mathbf{f}$ act on an object such that the object is in stable equilibrium (see Fig.6.1). By the assumptions given by above section, we can consider $\mathbf{f}$ to be distributed along the y axis, i.e. $\mathbf{f}(y) = (f_v(y), f_t(y))^T$, where $f_v(y)$ and $f_t(y)$ are the vertical and tangential component of $\mathbf{f}(y)$, $y \in [-A, A]$, where A is the half-width of fingertip. Then the sum of forces and sum of moments with respect to point o are 0, i.e.

$$\mathbf{F}_e + \int_{-A}^{A} \mathbf{f}(y)dy = 0 \tag{6.1}$$

and

$$\mathbf{r}_c \times \mathbf{F}_c + \int_{-A}^{A} y\mathbf{f}(y)dy = 0 \tag{6.2}$$

Denoting the equivalent concentrated force by $\mathbf{F} = (F_v, F_t)^T$, from (6.1) we have

$$F_v = \int_{-A}^{A} f_v(y)dy \tag{6.3a}$$

$$F_t = \int_{-A}^{A} f_t(y)dy \tag{6.3b}$$

The angle of the force with respect to the surface normal is

$$\alpha = tan^{-1}\frac{F_t}{F_v} \tag{6.4}$$

Since we have assumed that $\mathbf{f}$ is distributed along the y axis, the moment due to tangential components can be omitted. Then from (6.2) the exerting point of equivalent concentrated force, y^*, satisfies

$$y^* F_v = \int_{-A}^{A} y f_v(y)dy$$

or

$$y^* = \frac{\int_{-A}^{A} y f_v(y)dy}{\int_{-A}^{A} f_v(y)dy} \tag{6.5}$$

Using above method, the side contact between the fingertip and the object can be simplified as point contact with friction by changing l_2, θ_2 into l_2', θ_2' (see Fig.6.1).

It should be noted that under above simplicity, the length of l_2' and the angle θ_2' can be calculated from the location of y^* or, more precisely, from the information detected by tactile senors. By the assumptions in above section, this link can still be considered as rigid. Moreover, if a coordinate frame (O, X, Y) is set as shown in Fig.6.1, the representation of $\mathbf{F}$ in (o, x, y) can be easily transformed to (O, X, Y). In next section, we will use this simplified contact to study the static problem in a multifingered hand system.

6.3 The Statics Problem in a Multifingered Hand System

The static problem of a manipulator with one chain is to find the relationship between the generalized forces at the end-effector, $\mathbf{f}_{3\times 1}$, and the motor torques at the joints of the links, $\tau_{n\times 1}$, where n is the number of links. It is known that this relationship is described by

$$\tau = J^T \mathbf{f}, \tag{6.6}$$

where $J \in R^{3\times n}$ is Jacobian matrix of the manipulator. Using above equation one can easily calculate what torques the motors should apply at the joints to produce a desired force at the tip. The static problem of multifingered hand system is to determine the relationship among the torques that the motors should apply at the joints of links of the fingers, the desired grasping force and the resultant external force and torque exerted on the grasped object when the grasped object is in a stable equilibrium state.

Using the simplifying assumption of the previous section, the planar multifingered hand system with two fingers and two links for every finger can be shown as Fig.6.2.

In Fig.6.2, $L : (O_l, X_l, Y_l)$ and $R : (O_r, X_r, Y_r)$ are coordinate systems fixed on the tips of left and right finger, respectively; $P : (O_p, X_p, Y_p)$ is the coordinate

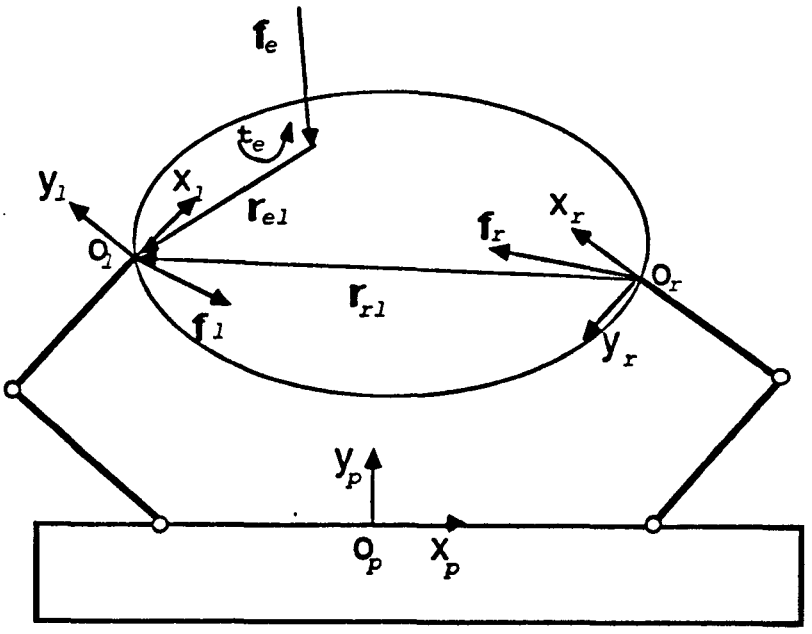

Fig.6.2 Two finger grasping

system fixed on the palm of the hand; $\mathbf{f}_l$ and $\mathbf{f}_r$ are the equivalent concentrated contact forces; $\mathbf{f}_e$ and $\mathbf{t}_e$ are the external force and torque exerting on the object, respectively; $\mathbf{r}_e$ is the vector from the point B, where $\mathbf{f}_e$ exerts, to O_l; $\mathbf{r}_{rl}$ is the vector from O_r to O_l.

From the basic statics, to keep the object in an equilibrium state, the net force and the net moment acting on it should be zero, respectively, i.e.

$$\mathbf{f}_l + \mathbf{f}_r + \mathbf{f}_e = 0 \tag{6.7}$$

and, if the reference point is chosen as O_l,

$$\mathbf{r}_{rl} \times \mathbf{f}_r + \mathbf{r}_e \times \mathbf{f}_e + \mathbf{t}_e = 0 \tag{6.8}$$

where " $\times$ " is the cross product of the vectors.

It is obvious that, Eq.(6.7) and (6.8) can only describe the state of the grasped object, but can not describe the state of the hand system completely

because there is redundancy in these equations. This redundancy can be explained as follows. Suppose $\mathbf{f}_e = 0$ and $\mathbf{t}_e \neq 0$. Decomposing $\mathbf{f}_r$ into two components, $\mathbf{f}_r^{\perp}$ and $\mathbf{f}_r^{\parallel}$, where $\mathbf{f}_r^{\perp}$ is perpendicular to $\mathbf{r}_{rl}$ and $\mathbf{f}_r^{\parallel}$ parallel to it. Similarly, $\mathbf{f}_l$ is decomposed into $\mathbf{f}_l^{\perp}$ and $\mathbf{f}_l^{\parallel}$. Then the scalar forms of Eq.(6.7) and (6.8) are

$$\mathbf{f}_l^{\perp} + \mathbf{f}_r^{\perp} = 0$$

$$\mathbf{f}_l^{\parallel} + \mathbf{f}_r^{\parallel} = 0$$

$$\mathbf{f}_r^{\perp} \times \mathbf{r}_{rl} + \mathbf{t}_e = 0$$

It is clear that the solution of $\mathbf{f}_l^{\parallel}$ and $\mathbf{f}_r^{\parallel}$ is not unique. However, if a constraint is set for the magnitude of $\mathbf{f}_l^{\parallel}$ or $\mathbf{f}_r^{\parallel}$ the solution will be unique.

To completely describe the two-fingered hand system, we define the *grasping force*, f_g as a scalar which equals the sum of magnitudes of the projections of finger-contact force on the line connecting two contact points minus the magnitude of projection of net external force on the same line. The admissible range of value of this quantity is prespecified depending on the requirement of the task, the material of the grasped object and the fingers (including the tactile sensors). By using this concept, the forces $\mathbf{f}_l, \mathbf{f}_r$ and $\mathbf{f}_e$ should satisfy

$$|\mathbf{r}_{rl} \cdot \mathbf{f}_l| + |\mathbf{r}_{rl} \cdot \mathbf{f}_r| - |\mathbf{r}_{rl} \cdot \mathbf{f}_e| = f_g \tag{6.9}$$

where " $\cdot$ " is the point product of the vectors. For grasping, the direction of $\mathbf{f}_l$ and $\mathbf{f}_r$ must be towards the interior of the object. According to the direction of r_{rl} we chose, Eq.(6.9) becomes

$$-\mathbf{r}_{rl} \cdot \mathbf{f}_l + \mathbf{r}_{rl} \cdot \mathbf{f}_r - |\mathbf{r}_{rl} \cdot \mathbf{f}_e| = f_g \tag{6.10}$$

Before expressing Eq.(6.7), (6.8) and (6.10) as the scalar equations, we discuss the transformation of the coordinates of L, R, and P. From Paul(1981), we know that for any point p, if its expressions of homogeneous coordinate in L, R, and P are $r^l = (x_l, y_l, 1)^T, r^r = (x_r, y_r, 1)^T$ and $r^p = (x_p, y_p, 1)^T$, then the homogeneous transformations from P to L and R are

$$r^l = T_p^l r^p \tag{6.11}$$

and

$$r^r = T_p^r r^p \tag{6.12}$$

respectively. In equations (6.11) and (6.12), the matrices T_p^l and T_p^r in $R^{3\times3}$ have the form:

$$T_p^l = \begin{pmatrix} A_{pl} & b_{pl} \\ 0 & 1 \end{pmatrix}$$

and

$$T_p^r = \begin{pmatrix} A_{pr} & b_{pr} \\ 0 & 1 \end{pmatrix}$$

where A_{pl} and A_{pr} in $R^{2\times2}$ are matrices of rotation transformation, b_{pl} and b_{pr} in R^2 are vectors of translation transformations. From Eq.(6.11) and (6.12), the homogeneous transformation from R to L is

$$r^l = T_r^l r^r = T_p^l T_r^p r^r \tag{6.13}$$

where

$$T_r^p = (T_p^r)^{-1} = \begin{pmatrix} A_{pr}^{-1} & -A_{pr}^{-1} b_{pr} \\ 0 & 1 \end{pmatrix}$$

$$T_r^l = \begin{pmatrix} A_{rl} & b_{rl} \\ 0 & 1 \end{pmatrix}$$

in which $A_{rl} = A_{pl}A_{pr}^{-1}$ and $b_{rl} = -A_{pl}A_{pr}^{-1}b_{pr} + b_{pl}$ are rotation and translation transformation from R to L, respectively.

Next, we will represent vector equations (6.7), (6.8) and (6.10) as scalar equations, in which every vector is presented in the coordinate system L. Let f_l^l and f_r^r in R^2 be representations of $\mathbf{f}_l$ and $\mathbf{f}_r$ in the coordinate systems L and R, respectively. Let f_e^p be the representation of $\mathbf{f}_e$ in the coordinate system P. Then the scalar expression of Eq.(6.7) is

$$f_l^l + A_{rl}f_r^r + A_{pl}f_e^p = 0 \tag{6.14}$$

Let r_e^p be the homogeneous coordinates of points B represented in P. Then the representation of the homogeneous coordinates of $\mathbf{r}_e$ in L is

$$r_e^l = -T_p^l r_e^p \tag{6.15}$$

Directly applying Eq.(6.13), the representation of homogeneous coordinates of $\mathbf{r}_{rl}$ in L is

$$r_{rl}^l = -T_r^l \begin{pmatrix} 0 \\ 0 \\ 0 \\ 1 \end{pmatrix} = (A_{pl}A_{pr}^{-1}b_{pr} - b_{pl}, 1)^T \tag{6.16}$$

Define a row vector, $S(r)$, for $r = (x, y, 1)^T$ as

$$S(r) = (-y, x) \tag{6.17}$$

Then the scalar expression of Eq.(6.8) is

$$S(r_{rl}^l)A_{rl}f_r^r + S(r_e^l)A_{pl}f_e^p + t_e = 0 \tag{6.18}$$

Define a row vector, $T(r)$, for $r = (x, y, 1)^T$ as

$$T(r) = (x, y) \tag{6.19}$$

Then the scalar expression of Eq.(6.10) is

$$-T(r_{rl}^l) f_l^l + T(r_{rl}^l) A_{rl} f_r^r + |T(r_{rl}^l) A_{pl} f_e^p| = f_g \tag{6.20}$$

In the rest of this section, we will derive the equilibrium equations expressed by the motor torques at the joints of the fingers and the external force and moment. Let τ_l and τ_r in R^2 denote the motor torques on the left and right fingers, respectively. From Eq.(6.6), we have

$$f_l^l = J_l^{-T} \tau_l \tag{6.21}$$

and

$$f_r^r = J_r^{-T} \tau_r \tag{6.22}$$

where J_l and J_r are Jacobian matrices of left and right finger, respectively. The inverse of them exists if and only if the joint angle between two links for every finger is not zero (Horn 1979). Substituting Eq.(6.21) and (6.22) to (6.14), (6.18) and (6.20), we have

$$\begin{pmatrix} J_l^{-T} & A_{rl} J_r^{-T} \\ 0 & S(r_{rl}^l) A_{rl} J_r^{-T} \\ -T(r_{rl}^l) J_l^{-T} & T(r_{rl}^l) A_{rl} J_r^{-T} \end{pmatrix} \begin{pmatrix} \tau_l \\ \tau_r \end{pmatrix} = \begin{pmatrix} A_l f_e^p \\ S(r_e^l) A_l f_e^p + t_e \\ f_g - |T(r_{rl}^l) A_l f_e^p| \end{pmatrix} \tag{6.23}$$

or briefly,

$$J\tau = \mathcal{F}_e \tag{6.23}'$$

It can be proved that the inverse of matrix J exists. In fact, we can rewrite J as

$$J = \begin{pmatrix} I & I \\ 0 & S(r_{rl}^l) \\ -T(r_{rl}^l) & T(r_{rl}^l) \end{pmatrix} \begin{pmatrix} J_l^{-T} & 0 \\ 0 & A_{rl} J_r^{-T} \end{pmatrix} = J_1 J_2 \qquad (6.24)$$

The inverse of second matrix of (6.24), J_2, obviously exists. From linear algebra, we know that if a square matrix has the form

$$\begin{pmatrix} A & B \\ C & D \end{pmatrix}$$

where A and D are square and $\det(A) \neq 0$, then its determinant is

$$det(A) det(D - CA^{-1}B)$$

Appling above result to the first matrix of (6.24), J_1, its determinant is

$$det(J_1) = det \begin{pmatrix} S(r_{rl}^l) \\ 2T(r_{rl}^l) \end{pmatrix}$$

By the definitions of $T(\cdot)$ and $S(\cdot)$, it is clear that $det(J_1) \neq 0$. Therefore, if the external force and moment and the position of point B with respect to coordinates system P are known, we can use Eq.(6.23) to obtain the motor torques to keep the grasped object in static state with required grasping force.

CHAPTER

SEVEN

CONCLUSION

In this thesis, we derived the basic relationship between the distribution of force exerted on the boundary of an elastic half-space and the distribution of stress or strain beneath the surface. This relationship is described by an integral equation of convolution type with two unknown functions. By noticing that the discrete Fourier transformation of the kernel for both stress and strain is real and nonnegative, we were able to use the DFT approach to solve the equation. Under some assumptions about friction, we use same approach to solve the corresponding inverse problem in the presence of tangential surface force. We noticed that the integral equation of convolution type with two unknown functions is the particular case of an operator equation of the first kind and that it is ill-posed on the natural function space for the problem. We developed an algorithm to solve it for two unknown functions by assuming that the distribution of strain or stress can be measured in two orthogonal directions. The two approaches above have been examined by examples. During the calculation of these examples, we found that above approaches are in their original form unsuitable for real time calculation. Hence, we also investigated the possibility of realizing analog networks to solve the inverse problem. Finally, as an application of tactile sensors, we derived the equation which expresses the relation of

the motor torques on the joints of the fingers and the external force exerted on the grasped object. In this equation, the contact force distribution measured by tactile sensors is simplified as an equivalent concentrated contact force.

The results given in this thesis are just preliminary ones. There is a number of problems left to be solved. With regard to the elastic model, we have not determined stress and strain for general three-dimensional contact. We expect that this model can be expressed as a double convolution of point contact. Moreover, in practice, the applied elastic material is not a half space, but a thin layer. Hahn and Levinson (1974) gave some results for this problem, but the form of their solution is an infinite series and inconvenient for applications. It would be interesting to recast their results in an integral form. Regarding the DFT approach, we did not find an algorithm to solve the inverse problem for the general case. The reason is that $\hat{K}_{x2}$ is an odd function. With regard to the regularization approach, an algorithm for finding the optimal regularization parameter has to be produced. Bates, Lindstrom, Wahba and Yandell (1987) gave a program for this problem, but it has to be modified for our stabilizing functional. With regard to the analog networks, to realize a real circuit for the inverse problem, many implementation questions have to be addressed.

BIBLIOGRAPHY

Bates, D. M., Lindstrom, M. J. Wahba, G. and Yandell, B. 1987,

GCVPACK-routines for generalized cross validation,

Commun. Statist.-Simul., 16(1), 263-297.

Chen, C. 1979,

One-dimensional digital signal processing, Marcel Dekker, Inc.

Coway, H. D., et al 1966,

Normal and shearing contact stress in indented strips and slabs,

Int. J. Eng. Sci. 4: 343-359.

Fearing, R. S. and Hollerbach, J. M. 1985,

Basic solid mechanics for tactile sensing,

Inter. J. Robotics Research, vol. 4, No.3, Fall.

Guillemin, E. A. 1963,

Theory of linear physical systems, New York, Wiley.

Hadamard, J. 1923,

Lectures on the Cauchy problem in linear partial differential equations,

New Haven: Yale University Press.

Hahn, H. T. and Levinson, M. 1974,

Indentation of an elastic layer bounded to a rigid cylinder. I.,

Int. J. Mech. Sci. 16: 480-502.

Hilgers, J. W. 1973,

Non-iterative methods for solving operator equations of the first kind,

Ph.D thesis, University of Wisconsin-Madsion.

Horn, B. K. P. (1979)

Kinematics, statics and two-dimensional manipulators,

in *Artificial Intelligence: An MIT perspective, edited by Winston, P. H.*

The MIT Press, 273-308.

Ivanov, V. K. 1962,

On linear problems which are not well-posed,

D. A. N. SSSR. 145 No. 2, 270-272.

Jensen. R. W. 1974,

Network analysis, Prentice-Hall, Inc.

Overton, K. J. and Williams, T. D. 1983,

Tactile sensation for robots: overview and experience,

Int. Computers in Engineering Conference and Exhibit vol 2. 155-123

Paul, R. P. 1981,

Robot manipulators: Mathematics, programming, and control,

The MIT Press.

Phillips, J. R. and Johnson, K. O. 1981,

Tactile spatial resolution. III. A continuum mechanics model of skin

predicting mechanoreceptor response to bars, edges, and grating,

J. Neurophys. 46(6):1204-1225.

Poggio, T. and Koch. C. 1985,

Ill-posed problems in early vision:

from computational theory to analogue networks,

Proc. R. Soc. London B 226, 303-323.

Salisbury, J. K. 1982,

Kinematic and force analysis of articulated hands,

Ph. D. Thesis, Stanford University.

Tikhonov, A. N. and Arsenin, V. Y. 1977,

Solutions of ill-posed problems, John Wiley and Sons.

Timoshenko, S., and Goodier, J. N. 1951,

Theory of elasticity, New York: McGraw-Hill.

CURRICULUM VITAE

Name: Rui Yang

Permanent Address: c/o Prof. Jiachi Yang
Building 13, No. 304
Zhong Guan Cun
Beijing, P. R. China

Degree and date to be conferred: M.S., 1987.

Date of birth: September 4, 1957

Place of birth: Beijing, P.R. China

Secondary education: Qing Hua Yuan Middle School, Beijing, P. R. China

Collegiate institutions attended:	Dates	Degree	Date of Degree
University of Maryland College Park, Maryland	09/85 - 08/87	M.S.	08/87
Changsha Institute of Engineering Changsha, P. R. China	01/78 - 12/81	B.S.	12/81

Major: Electrical Engineering.